



Combined thermochemical-biotechnological approach for the valorization of polyolefins into polyhydroxyalkanoates: Development of an integrated bioconversion process by microbial consortia

Passanun Lomwongsopon^a, Tanja Narancic^b, Reinhard Wimmer^c, Cristiano Varrone^{a,*}

^a Section of Bioresources and Process Engineering, Department of Chemistry and Bioscience, Aalborg University, Fredrik Bajers Vej 7H, 9220, Aalborg, Denmark

^b School of Biomolecular and Biomedical Science, And BiOrbic - Bioeconomy Research Centre, Ireland, University College Dublin, Belfield, Dublin 4, Ireland

^c Section of Medical Biotechnology, Department of Chemistry and Bioscience, Aalborg University, Fredrik Bajers Vej 7H, 9220, Aalborg, Denmark

HIGHLIGHTS

- PO wax-degrading MMCs were developed via enrichment and adaptive laboratory evolution.
- MMC consumed >80% of PO wax in 12 h, 4 times faster than what have been reported.
- MMC bioconversion can upcycling PO wax to triglycerides and PHAs.
- Statistical optimization improved PHAs titer to 384.09 mg L⁻¹ (5.6X increased).
- Maximum %PHA per cell biomass can be pushed to ~35% using C/N of 94.52.

GRAPHICAL ABSTRACT



ARTICLE INFO

Handling editor: Yongmei Li

Keywords:

Bioconversion
Microbial mixed consortia
Plastic upcycling
Polyethylene
Polyhydroxyalkanoates
Triglycerides

ABSTRACT

Waste management of persistent polymers such as polyolefins (PO)¹ still represents a major challenge, often leading to material loss from the value chain and contributing to plastic pollution. This study investigated an integrated process to valorize PO pyrolysis side stream. PO wax was recovered and used as a feedstock for a microbial bioconversion process. A modified emulsification protocol (using two-surfactants system) allowed the successful dispersion and bioconversion of PO wax without the need of the extra oxidation step. Enrichment of plastic landfill inocula allowed to develop efficient mixed microbial consortia (MMC) able to grow on PO wax. Adaptive laboratory evolution improved 4 times cell growth, leading to 2.6–17.3 times shorter lag phase. The bioconversion process using the adapted MMC was performed in a 2 L-bioreactor with PO wax-emulsified media (10 g L⁻¹) at neutral pH and 20% pO₂. 87% of substrate was consumed within 12 h and complete consumption was achieved within 48 h (4 times faster than previously reported). A maximum of 2.95 g_{CDW} L⁻¹ of biomass was produced, while the intracellular triglycerides reached a maximum of 105.5 mg L⁻¹ at 30 h. Moreover, the conversion of PO wax into polyhydroxyalkanoates (PHAs) was demonstrated and the production was maximized by statistical optimization. Maximum PHA titer of 384.09 mg L⁻¹ was achieved, which represents a 1.5–17 times improvement from previous reports. This integrated thermochemical-biotechnological approach might represent

* Corresponding author.

E-mail address: cva@bio.aau.dk (C. Varrone).

<https://doi.org/10.1016/j.chemosphere.2024.143671>

Received 22 September 2024; Received in revised form 24 October 2024; Accepted 1 November 2024

Available online 5 November 2024

0045-6535/© 2024 The Authors. Published by Elsevier Ltd. This is an open access article under the CC BY license (<http://creativecommons.org/licenses/by/4.0/>).

an interesting strategy to valorize and upcycle currently unrecyclable PO-rich mixed plastic waste streams, thus improving the circularity of the plastic sector.

1. Introduction

The relentless growth of plastic production worldwide requires the use of large quantities of fossil resources and generates a huge amount of post-consumer waste. The inefficiency of current recycling processes toward plastic mixtures and blends, multilayers, and food-contaminated plastic waste often leads to a linear life cycle (produce, use, discard), with a consequent loss of materials. Out of 460 Mt of plastics produced worldwide in 2019, only 9% was ultimately recycled while 19% was incinerated, 50% was sanitarily landfilled, and the rest was disposed in uncontrolled dumpsites and leaked into the environment (OECD, 2022). To implement a more sustainable value chain of plastic, the European Commission has adopted the EU Strategy for Plastics in a Circular Economy to ensure that plastics have end-of-life with reusing and/or recycling options (European Commission, 2020). Valorizing plastic waste through its use as a feedstock to produce higher-value products represents an important strategy to reach these goals (Roux and Varrone, 2021).

Polyolefins (PO) makes up approximately 45% of plastic production in Europe (26% of polyethylene (PE) and 19% of polypropylene (PP)), mainly used in the packaging sector (PlasticsEurope, 2023). It is a very high molecular weight plastic with C-C bonds that is very recalcitrant toward (bio)degradation, thus persisting in the environment for a very long time (Chamas et al., 2020). Mechanical recycling can be applied to process post-consumer PO; however, there is a limitation toward contaminated streams and blends (Garcia and Robertson, 2017). Pyrolysis is one of the chemical recycling technologies that yields hydrocarbons, which can be used as feedstock in the petrochemical industry, and allows for heat recovery from plastic waste (plastics-to-fuels). Pyrolysis of PE produces a high amount of waxes, in addition to gases and oils, especially at moderate temperatures and operating pressures (Al-Salem and Dutta, 2021). PE wax is mostly used in low-value applications, e.g., coatings and lubricants, or is upgraded in petroleum refineries (Al-Salem et al., 2020). The main composition of PE wax is a mixture of aliphatic hydrocarbons from C8-C32, mainly alkanes (Guzik et al., 2014), which, contrary to polymeric PE, are a metabolizable substrate for microorganisms that possess specific enzymes. PP wax was reported to be made primarily of alkenes, and the amount of waxes depends on the catalysts used (alkaline catalysts yielded >80% of waxes) (Tekin et al., 2012; Yao et al., 2019). Integrating microbial conversion to valorize PO pyrolysis wax into higher-value products can thus allow the upcycling of thermal deconstructed plastic waste.

Only a few studies have investigated the integrated thermochemical and biotechnological approach to upcycle PO to some valuable products, including polyhydroxyalkanoates (PHAs) (Guzik et al., 2014, 2021; Johnston et al., 2017; Radecka et al., 2016), wax esters (Gregory et al., 2023), triglycerides (Torres-Zapata et al., 2022), and microbial proteins (Byrne et al., 2022).

PHAs are biodegradable aliphatic polyesters that have the substitutable properties to petroleum-based plastics, making them an excellent environmentally friendly alternative as bioplastics (Park et al., 2024). Short-chain-length PHAs (scl-PHAs), such as poly(3-hydroxybutyrate) (PHB) and poly(3-hydroxybutyrate-co-3-hydroxyvalerate) (PHBV), are used for food packaging and single-use items (Kourmentza et al., 2017). Medium chain length polyhydroxyalkanoates (mcl-PHAs), which are elastomers, are highly suitable for medical applications such as suture materials, soft tissue engineering, and drug delivery matrices (Hahn et al., 2024; Kourmentza et al., 2017; Pereira et al., 2019). Upcycling PO wax to PHAs not only manages the most abundant post-consumer plastic waste but also produces bioplastics from recycled feedstock. *Pseudomonas aeruginosa* GL-1 and PAO1 were

able to grow on 0.05% (w/v) PE pyrolysis wax with a cell dry weight (CDW) of 0.19–0.23 g L⁻¹ and PHA production of a maximum 9.8% CDW in 48 h. Addition of a biosurfactant (0.05% (w/v) rhamnolipids) enhanced growth to 0.31–0.39 g_{CDW} L⁻¹ and PHA accumulation to 14.5–18.9% CDW (Guzik et al., 2014). Later, the same research group improved the efficiency of the PHA production process from PE pyrolysis wax by integrating chemical oxidation to convert PE wax to a PE wax-derived fatty acid mixture, which was used as the carbon source for PHA fermentation by *Pseudomonas putida* KT2440. In a 20-L bioreactor, they were able to produce 83 g_{CDW} L⁻¹ with 65% PHA in 25 h, which was significantly higher than shake flasks cultivation (0.17 g_{CDW} L⁻¹ with 25.2% PHA in 48 h) (Guzik et al., 2021). Nevertheless, this process used a high amount of energy and chemicals. Their report on cost estimation showed that integrating the chemical oxidation step increased costs by more than 13 times, and 80% of the total cost was spent on the solvent used in recovering fatty acids from the remaining unreacted hydrocarbons. Thus, an efficient and economically feasible process for PE bioupcycling still needs to be developed.

Aerobic biodegradation pathway of alkanes was shown to involve several oxidative enzymes that oxidize hydrocarbons to fatty acids, which will be further metabolized via β -oxidation (Ji et al., 2013; Rojo, 2010). Each of these enzymes has certain preferable chain lengths and types of hydrocarbons. For instance, methane monooxygenases, alkane monooxygenases, bacterial P450, and dioxygenases are typically involved in degradation of C1-C4, C5-C16, C5-C16, and C10-C30 saturated aliphatic hydrocarbons, respectively, while alkene monooxygenases and epoxide carboxylases convert unsaturated aliphatic hydrocarbons (Abbasian et al., 2015). Moreover, several other enzymes, e.g., alcohol and aldehyde dehydrogenases, are also involved in intermediate steps before fatty acid formation (Ji et al., 2013). Biotechnological processes employing the mixed microbial consortia (MMCs) can thus be more beneficial as the synergistic interaction between members of the consortia and their complementary metabolic pathways and enzymes are anticipated to promote the utilization of complex substrates better than single strains (Varrone et al., 2018). Such process could also help avoid the cost- and energy-intensive chemical oxidation step. In addition, as pyrolysis products' composition depends on the feedstock and pyrolysis reactor parameters, e.g., temperature, pressure, or catalyst usage (Christopher et al., 2023), MMC process have the additional advantage of being able to handle batch-to-batch variations of incoming substrates. The positive interactions between species in the consortia is expected to enhance the tolerance against toxicity and contaminations of the substrate (Piccardi et al., 2019).

Enrichment of the environmental inocula of microorganisms under defined conditions represents a conventional method to gain functional MMC. It alters original microbial proportions, selecting beneficial interactions or triggering new associations to improve the consortia's capabilities (Massot et al., 2022), based on the selective conditions applied. The enhancement of a microbial community performance can be done by adaptive laboratory evolution (ALE). ALE is typically employed as a valuable method for single strain improvement and optimization (Portnoy et al., 2011), but has also been shown to develop synergistic interaction in microbial consortia (Konstantinidis et al., 2021; Liu et al., 2019). Repeated cultivation under (increased) selective pressure, e.g., nutrient or environmental stress, can lead to phenotypic improvement and genotypic diversification, possibly because of the emergence of mutations (Dragosits and Mattanovich, 2013). In the essence of bioupcycling application, the development of robust functional MMC via enrichment and ALE could allow (pretreated) polymer consumption and bioconversion to valuable products to take place in a one-pot process, which would greatly reduce the process cost.

Even though PO are typically the main polymers in post-consumer mixed plastics, finding a viable and sustainable solution to handle such streams is still a major challenge. While efficient sorting would allow to mechanically recycle PO, this is not always possible (for instance in the case of multi-layers, compounded materials, contaminated packaging material, etc.), leading to an unrecyclable mixed plastic waste fraction. As these unrecyclable fractions can be subjected to pyrolysis, we developed a promising valorization strategy by integrating a biotechnological process using MMC to boost bioupcycling of PO pyrolysis wax into higher-value products. Functional MMC was developed through enrichment and ALE with a stepwise increase of (non-oxidized) PO wax concentration. Aim of this study was to develop a bioprocess by using the pyrolysis wax as it is, without an extra oxidation step, reducing the extra cost from supplying heat, oxygen/ozone, and chemicals in the catalytic reaction or the purification step. Extra- and intracellular products from the bioconversion process were analyzed to investigate different upcycling opportunities. Design of Experiment (DoE) was performed to optimize the PHA production. The developed process represents a strategy to recover carbon trapped in fossil-based plastic waste and convert into a more sustainable bioplastic.

2. Materials and methods

2.1. PO pyrolysis wax

The PO pyrolysis wax was provided by Waste Plastic Upcycling (WPU) Denmark and generated from mixed PO using a commercial pyrolysis process. Two different batches of PO pyrolysis wax were used during the experiments. The compositions were characterized by proton nuclear magnetic resonance (1H NMR) and gas chromatography–mass spectrometry (GC-MS). 1H NMR was used to determine the composition (aromatic, paraffinic, and olefinic). The wax samples were dissolved in deuterated chloroform at 30 mg mL⁻¹ and the solutions (0.6 mL) were transferred to 5 cm-NMR tubes. 1H NMR spectra were recorded at 600 MHz. The relative number of carbon atoms, classified as aromatic, paraffinic, and olefinic, in the samples was calculated from NMR integral spectra (after phase and baseline correction), according to the method reported by Myer et al. (Myers et al., 1975).

2.2. Microbial consortia enrichment and adaptive laboratory evolution

Soil and leachate samples used as start inoculum were collected from a plastic landfill located in Avedøre (Greater Copenhagen Area), Denmark. A mixture of all collected samples (10 g) was added to 100 mL of Maximum Recovery Diluent (1 g L⁻¹ peptone and 8.5 g L⁻¹ NaCl), stirred for 30 min, then allowed to settle for another 30 min (Montazer et al., 2018). The top liquid, containing mainly microorganisms without soil residues, was used as the inoculum for the flask-scale enrichment process.

0.5 g of PO pyrolysis wax was heated up in 29 mL distilled water at approximately 80 °C on a hot plate to melt the wax. Then, the wax suspension was sonicated for 7 min at 60% amplitude (30s on and 30s off interval) using Bandelin Sonoplus HD2200 sonicator (Berlin, Germany) to obtain a PO wax emulsion (Radecka et al., 2016). The emulsion was then transferred to a flask filled with 11 mL of concentrated Mineral Salt Media (MSM) components (to obtain the final concentrations of each component in 50 mL working volume according to Welsing et al. (2021)). NH₄(SO₄)₂ was used as a nitrogen source with the final concentration of 2 g L⁻¹. Three parallel flasks were prepared, and 10 mL of inoculum was added to each flask. The culture flasks were incubated at 30 °C and 150 rpm in a shaking incubator.

For the enrichment, a repeated transfer technique was used: eight cycles were performed by transferring a well-mixed subculture into new media at specific time intervals. The subculture was performed every 4 weeks during the first three cycles and every 2 weeks for the rest. ATP concentration of enrichment cultures was measured every week to track

the viability of the microbial consortia (BacTiter-Glo™ Microbial Cell Viability Assay, Promega, Madison, WI, USA). Growth curves of the consortia on 1% PO wax were obtained before and after the enrichment process, to compare their performances.

ALE was performed on the two best enriched consortia that had a relatively low lag phase on PO wax. The microbial consortia (10 mL) were inoculated into 250 mL-flasks containing 50 mL PO wax emulsified in MSM, prepared as mentioned earlier. Repeated transfers were done every 24–72 h (depending on the substrate concentration) during the exponential phase of the enriched consortia, starting from an Optical Density at 600 nm (OD₆₀₀) of 0.2. A stepwise increase of PO wax concentration from 1% to 6% (w/v) was used to adapt the consortium to higher substrate loadings, increasing the tolerance to higher wax concentrations. The growth curves of the ALE consortia were characterized and compared to the original consortia. The ALE was considered concluded when the transfer to a higher substrate concentration did not lead to a further improvement in the growth and metabolic activity. The consortia after ALE were stored at –80 °C in 30% glycerol prior to use in the following experiments.

2.3. Preparation of PO wax emulsion with two monomeric surfactants

The stability of the PO wax emulsion was improved by adding two monomeric surfactants, water-soluble Tween 20 and oil-soluble Span 80. 10 g PO wax was melted at approximately 80 °C and mixed together with 10 g mineral oil (light) (Sigma-Aldrich, Denmark) and 1 g Span 80 with a magnetic stirrer. In parallel, 780 mL distilled water was mixed with 1 g Tween 20 at approximately 85 °C. The wax/oil phase was added dropwise to the water phase under vigorous stirring on the magnetic stirrer. After the wax/oil phase was added, the mixture was kept stirring for 15 min more to pre-emulsify the content. Then, the mixture was sonicated for 10 min at 80% amplitude (30s on and 30s off interval) (Bandelin Sonoplus HD2200, Berlin, Germany).

2.4. Bioreactor cultivation of adapted consortia

The PO wax emulsion was mixed with the other components of MSM (nitrogen source, buffer, and trace elements solution) to 900 mL in the 2-L bioreactor (Sartorius Biostat® A), equipped with a temperature, pH, and dissolved oxygen (DO) control system. 100 mL of inoculum (pre-activated in shake flasks with 10 g L⁻¹ PE wax as a carbon source for 48 h, washed twice with MSM without carbon source, and adjusted to OD₆₀₀ = 1.0) was added to reach the working volume of 1 L with a wax concentration of 10 g L⁻¹ and a starter culture of 10% (v/v). The partial oxygen pressure (pO₂) was controlled at 20% by cascade control of aeration (0–2000 ccm) and stirring rate (250–650 rpm). The temperature was controlled by a heating jacket at 30 °C and the pH was kept at 7.0 with an alkali solution of NaOH (1 M). The cultivation was conducted for 48 h.

6 mL of the culture was withdrawn from the bioreactors at each time point for analysis. 200 µL was used in the hydrocarbon extraction process to analyze substrate consumption. The rest of the volume was used for measuring the growth of microbial consortia by OD₆₀₀ and CDW. The culture was centrifuged at 10000 rpm for 10 min. The cell pellets were washed with hexane to eliminate the remaining wax and oil. The resuspended cells in hexane were then centrifuged and the hexane was discarded. For OD₆₀₀ measurement, the cell pellet was re-suspended in distilled water and diluted to the required range (2–20X) before measurement. For CDW, the cell pellet was freeze-dried overnight (or until completely dried) to get rid of moisture and collected.

2.5. Statistical optimization of PHA production from PO wax

Response Surface Methodology (RSM) was employed to analyze the interactive effect of PO wax concentration (1–20 g L⁻¹), C/N ratio (5–100), and MMC inoculum size (1–20% v/v) on the responses, which

included PHA titer (mg L^{-1}) and yield ($\text{mg}_{\text{PHA}} \text{g}_{\text{PO}}^{-1} \text{wax}^{-1}$). Central Composite Design (CCD) was used to design the experiment, using Stat-Ease 360 (USA), resulting in 48 experimental conditions (runs) with 3 replicates and 6 center points. Multiple regression was used to analyze the experimental results by fitting quadratic polynomial model. Analysis of Variance (ANOVA) was performed on each model. The relationship between the response variables and the design variables were visualized with 3D response surface plots to predict the optimal conditions.

Preliminary tests: different nitrogen sources, including $\text{NH}_4(\text{SO}_4)_2$, NH_4Cl , NaNO_3 , and NaNO_2 , were firstly screened for the best suitability for PHA production media (contained 0.065 gN L^{-1} of nitrogen source, $9 \text{ g L}^{-1} \text{Na}_2\text{HPO}_4 \cdot 12\text{H}_2\text{O}$, $1.5 \text{ g L}^{-1} \text{KH}_2\text{PO}_4$, $200 \mu\text{g mL}^{-1} \text{MgSO}_4 \cdot 7\text{H}_2\text{O}$, $2 \text{ mg L}^{-1} \text{ZnSO}_4 \cdot 7\text{H}_2\text{O}$, $1 \text{ mg L}^{-1} \text{CaCl}_2 \cdot 2\text{H}_2\text{O}$, $5 \text{ mg L}^{-1} \text{FeSO}_4 \cdot 7\text{H}_2\text{O}$, $0.17 \text{ mg L}^{-1} \text{Na}_2\text{MoO}_4$, $0.2 \text{ mg L}^{-1} \text{CuSO}_4 \cdot 5\text{H}_2\text{O}$, $0.4 \text{ mg L}^{-1} \text{CoCl}_2 \cdot 6\text{H}_2\text{O}$, $1.22 \text{ mg L}^{-1} \text{MnCl}_2 \cdot 4\text{H}_2\text{O}$, and $10 \text{ mg L}^{-1} \text{EDTA}$). 10 g L^{-1} PO wax was used as a sole carbon source (emulsion with two monomeric surfactants without mineral oil) for the screening experiment. The cultivation was performed with the working volume of 25 mL at 30°C and 200 rpm for 48 h. Then, the cell biomass was collected and freeze-dried for CDW determination and subsequently PHA analysis.

2.6. Quantification of wax consumption by GC-MS

Samples from the bioreactors taken at various intervals were mixed with dichloromethane (DCM) at the volume ratio of 1:1 by shaking for 30 min. The extractions were centrifuged at 14000 rpm for 5 min for layer separation. The DCM layer was analyzed by GC-MS. The injection temperature was 350°C , column temperature program was 35°C (2 min), using a ramp at the rate of $25^\circ\text{C min}^{-1}$ to 100°C , then at the rate of $50^\circ\text{C min}^{-1}$ to 350°C and hold at 350°C (6.5 min). The detection temperature was 300°C . The products were identified by a GC (Agilent Intuvo 9000) equipped with an Agilent DB-5ms column ($30 \text{ m} \times 250 \mu\text{m} \times 0.25 \mu\text{m}$) and a high-resolution MS (Agilent 7010B Triple Quadrupole) with liquid injection field desorption ionization. For peak identification, the standard solution containing alkane from C7 to C40 (Sigma-Aldrich, Denmark) was used, with the help of the NIST library in some of the unknown peaks.

2.7. Intracellular triglycerides analysis

Intracellular triglycerides were analyzed according to the protocol reported by a previous study (Torres-Zapata et al., 2022). Freeze-dried biomass (50 mg) was resuspended in 1 mL of acidic methanol (methanol: sulfuric acid at 97.5: 2.5 v/v). The samples were incubated in a thermoshaker at 900 rpm and 80°C for 1.5 h to transform triglycerides into fatty acid methyl esters (FAMES). 1.5 mL of water was added to the tube to terminate the reaction, followed by the addition of 0.5 mL hexane. The tubes were vortexed vigorously for approximately 3 min to extract the FAMES into the hexane phase. Then, the phase separation was performed by centrifuging at 14000 rpm for 5 min. 200 μL of the hexane phase was transferred to the glass vials for subsequent analysis of FAMES by GC-FID.

GC equipped with a ZB-FAME column ($30 \text{ m} \times 250 \mu\text{m} \times 0.20 \mu\text{m}$) and a flame-ionization detector (FID) was used to analyze FAMES. Helium was used as a carrier gas at the constant flow rate of 1.0 mL min^{-1} . The injection was performed with a split mode with a split ratio of 50:1. The injection temperature was 270°C . The oven program started with a temperature of 125°C , ramped to 240°C at the rate of 5°C min^{-1} , and held for 9 min. The FAMES standard (Supelco 37 Components FAMES mix, Sigma-Aldrich, Germany) was used to identify and quantify bacterial intracellular triglycerides.

2.8. PHA analysis

The PHA content (%PHA per CDW) and PHA monomer composition were analyzed by acidic methanolysis of dried cell biomass as described

by Brandl et al. (1988). Freeze-dried biomass (5–10 mg) was resuspended in 1.5 mL of acidic methanol (methanol: sulfuric acid at 5: 1 v/v) and 1.5 mL of chloroform with methyl benzoate (as an internal standard). The samples were incubated at 100°C for 3 h and, after that, cooled down on ice. Then 1 mL of water was added to the tube to terminate the reaction, and the chloroform phase was transferred to the glass vials for GC-FID analysis of 3-hydroxyalkanoic acid methyl esters.

The same GC condition and column as for FAMES analysis was used for PHA, though with a different heating program (start temperature of 120°C for 5 min, ramped to 180°C at the rate of $10^\circ\text{C min}^{-1}$ and held for 1 min, then ramped to 250°C at the rate of $10^\circ\text{C min}^{-1}$ and held for 5 min).

2.9. 16s rRNA sequencing of microbial consortia composition

Total genomic DNA was extracted from the enriched mixed consortia (1 mL) using the DNeasy PowerBiofilm Kit (Qiagen, Hilden, Germany) according to the manufacturer's instructions. After the extraction, Qubit and Nanodrop (ND2000) were used to check the concentration and the purity of the isolated DNA. In addition, agarose gel electrophoresis was performed to check the quality of the DNA before library preparation. 16s full-length amplicons were sequenced on PacBio Sequel II/IIe. Amplicon Sequence Variants (ASVs) analysis and species annotation were performed to reveal microbial composition in the enriched consortia.

3. Results and discussion

3.1. PO pyrolysis wax composition

Characterization of the PO pyrolysis wax used in this study was performed by $^1\text{H NMR}$ and GC-MS. In $^1\text{H NMR}$ spectra, peaks indicating methyl group of alkanes, methylene groups of alkanes, methine groups of alkanes, α -methyl groups of aromatics, ring's proton of aromatics, and olefinic protons of alkenes were integrated at the chemical shifts of 0.6–1.0, 1.0–1.5, 1.5–2.0, 2.0–3.0, 6.6–8.0, and 4.5–6.0 ppm, respectively. Fig. 1a and b summarizes the fractions of different hydrocarbon types in two different batches of PO wax samples. The profiles of alkanes and alkenes were further revealed by GC-MS (Fig. 1e and f). From a physical inspection, the first batch of PO wax samples (Fig. 1c) used in this study was softer and less solid than the second batch (Fig. 1d). Consequently, the distribution of hydrocarbons showed a higher proportion of longer chains (C26–C39) in the second batch (Fig. 1f), compared to the first batch (Fig. 1e). As previously reported, 83.2% of the total composition of heavy wax from mixed plastic waste from landfill pyrolyzed at 500°C is hydrocarbons of $\text{C} \geq 20$ (Al-Salem et al., 2020). In addition, the first batch had higher alkene proportions. Pyrolysis product distribution is affected by the pyrolysis reactor parameters, for instance, temperature, feedstock, time, catalyst, and catalyst/plastic ratio (Christopher et al., 2023), as well as the variability of the plastic feedstock used. Thus, batch-to-batch variations can be expected. Batch 1 of PO wax was used during the enrichment and ALE of microbial consortia, whereas batch 2 was used during the bioreactor cultivation. The high variability observed among batches underlines even more the importance of using robust microbial mixed consortia rather than pure strains.

3.2. Enrichment of PO wax-degrading microbial consortia and the microbial diversity analysis

Samples collected from the plastic landfill were pooled together and enriched on PO pyrolysis wax emulsion for 5 months. The enrichment was stopped when the ATP concentration at the end of the cycle did not improve anymore (Fig. S1). The growth curve data of the three enriched consortia, named as W1, W2, and W3, on 10 g L^{-1} PO wax were collected over 13 d (Fig. 2a). The data showed a clear growth

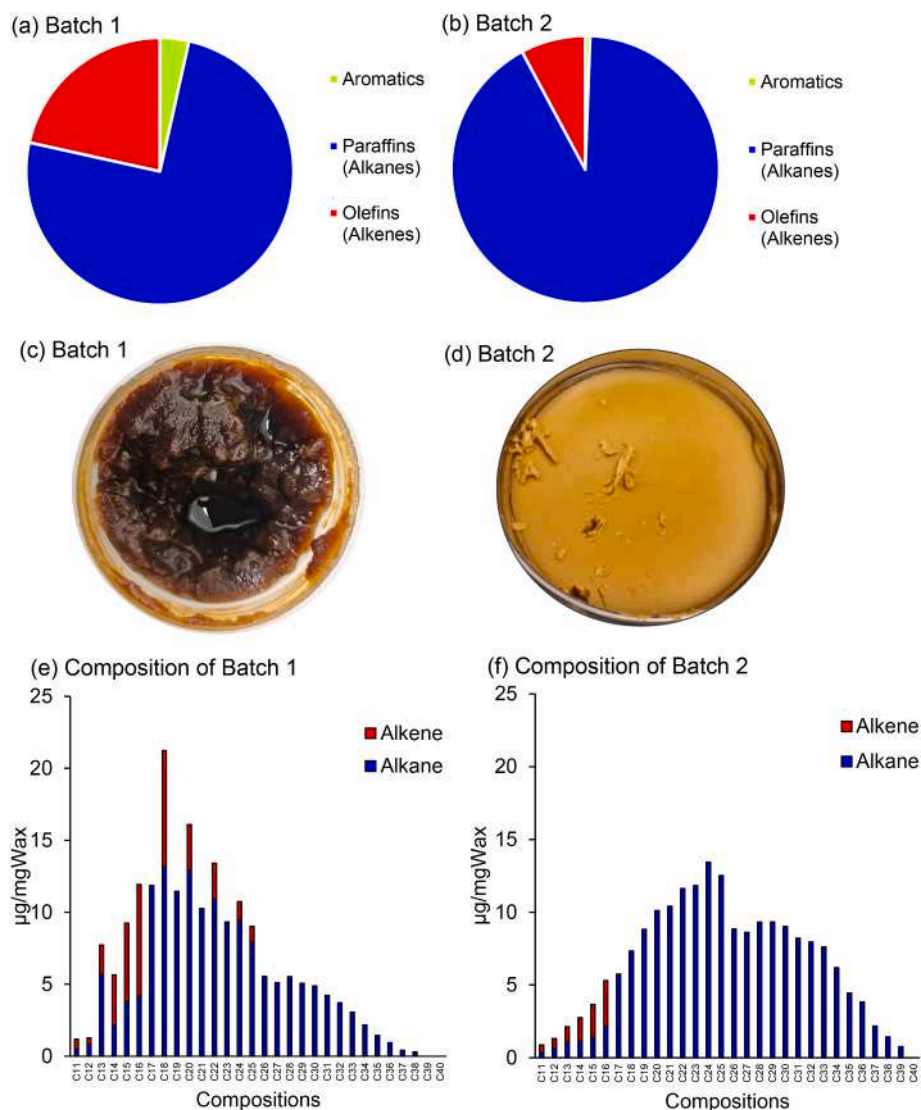


Fig. 1. Compositions of two different batches of PO pyrolysis wax analyzed by 1H NMR (a, b), physical appearances (c, d), and hydrocarbon distributions (e, f): Batch 1 (a, c, e) and Batch 2 (b, d, f).

improvement after enrichment compared to the original inoculum. Applying the bacterial growth curve model from Zwietering (Zwietering et al., 1990) to the experimental data shows that consortia W1 and W2 had a shorter lag phase on PO wax compared to W3 (2.8 and 22.5 h, respectively) (Table 1). Consortium W3 could reach a higher OD600 than W1 and W2, after 260 h, but the lag phase was 17 and 2 times longer. Therefore, W1 and W2 were selected for subsequent microbial diversity analysis and ALE experiments.

To understand how enrichment shapes the microbial communities, 16s full-length amplicon sequencing was performed to characterize the bacterial community's structure at the genus level. Fig. 2b shows the genera with relative abundance greater than 1% in W1 and W2 communities, during enrichment cycle 0, 3, and 7 (T0, T3, and T7). The genera with less than 1% relative abundance were combined into the "others" category. At T0, W1 was composed of bacteria from several phyla with relatively similar proportions, including *Corynebacterium* (10.0%), *Tissierella* (6.3%), *Planctomicrobium* (14.6%), *Brevundimonas* (7.5%), *Aquamicrobium* (8.9%), *Alcaligenaceae* (11.3%), *Verticillia* (7.6%), and others. Whereas W2 had a high proportion of *Saccharimonadaceae* (26.5%), followed by *Gordonia* (13.2%), *Planctomicrobium* (10.3%), *Alcaligenaceae* (7.6%), *Brevundimonas* (6.5%), *Corynebacterium* (5.6%), *Ottowia* (4.6%), and others. After sub-culturing for 3 cycles (T3),

the communities' profiles were largely changed, but further sub-culturing to T7 only showed slight change. *Ottowia*, *Rhodococcus*, and *Gordonia* were dominant during T3 but decreased during T7 in consortium W1. W1 comprised mainly *Achromobacter*, *Stenotrophomonas*, *Ochrobactrum*, and *Camelimonas* in T7, while W2 mainly comprised *Stenotrophomonas* and *Sphingobacterium*. *Ochrobactrum* and *Achromobacter* represented 17.2% and 9.3% during T3 but decreased to 6.1% and 4.8% during T7 in consortium W2. A high relative abundance of genus *Achromobacter* (40.7%) was observed in W1, while *Stenotrophomonas* (57.4%) was observed in W2. Both genera are non-fermenting Gram-negative rod shaped bacteria that have been shown to degrade alkanes, diesel oil, and aromatic hydrocarbons (Behera et al., 2020; Deng et al., 2014; Gargouri et al., 2017; Hassanshahian et al., 2013; J. Li et al., 2020; Y. Li et al., 2020). They have been studied for their bioremediation potential of petroleum/crude oil/gasoline-contaminated environments. Production of biosurfactants was reported on some strains of *Achromobacter* and *Stenotrophomonas* (Deng et al., 2016; Gargouri et al., 2017; Kazemzadeh et al., 2020; J. Li et al., 2020). Even though both W1 and W2 consortia originated from the same start inoculum and developed similar functional consortia, the development over time was different. After all, outcomes of microbial community structure after enrichment could be affected by different factors, including subsampling (random

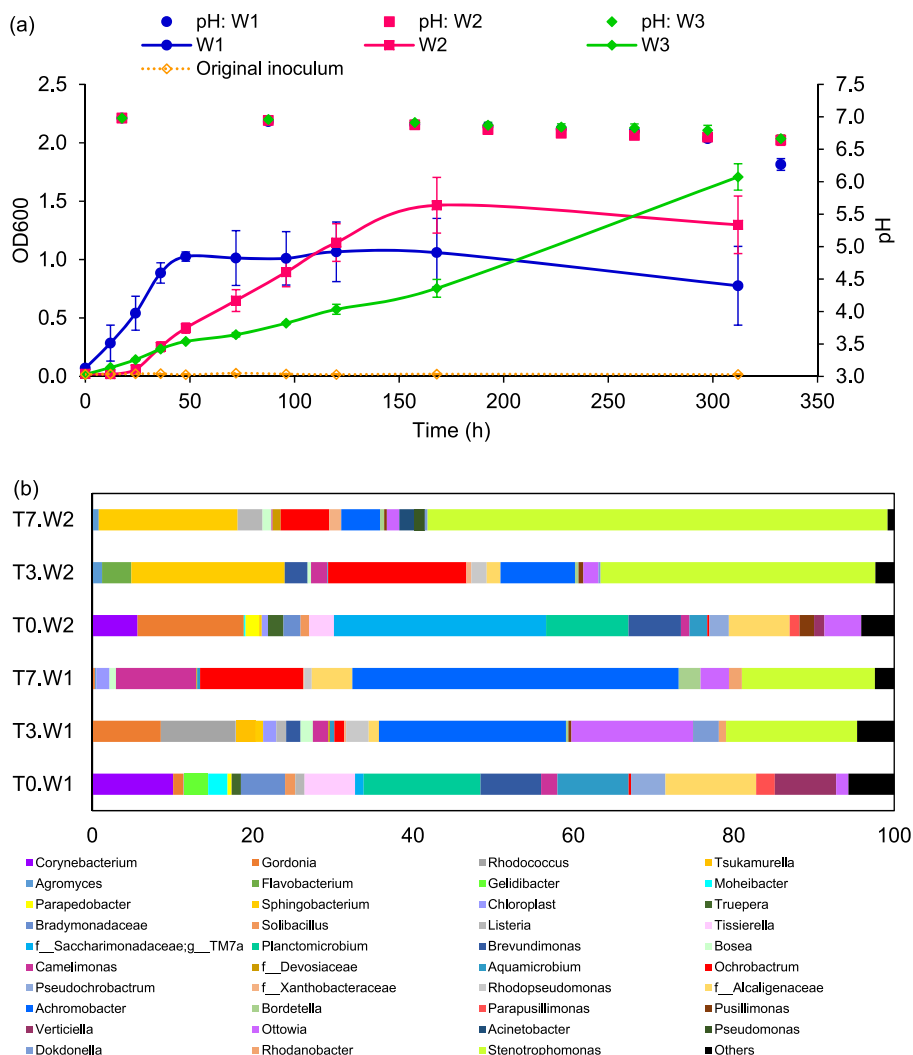


Fig. 2. Growth curves of three different enriched consortia (W1, W2, and W3) on 10 g L⁻¹ PO wax after enrichment in comparison with the original inoculum before enrichment (a); and microbial composition at a genus level of consortia W1 and W2 at different enrichment time (T0: original consortia, T3: after 3 cycles of transfers, T7: after 7 cycles of transfers) (b).

Table 1
Parameters derived from the growth curve by the Zwietering model fitting.

Consortium	Maximum OD600	Growth rate (h ⁻¹)	Lag phase (h)	R ²
Original inoculum	0.02 ± 0.00	0.01 ± 0.01	167.03 ± 0.00	0.946
W1	1.01 ± 0.26	0.04 ± 0.00	2.83 ± 2.59	0.823
W2	1.30 ± 0.29	0.01 ± 0.00	22.48 ± 2.42	0.958
W3	3.66 ± 1.83	0.01 ± 0.00	49.46 ± 35.22	0.987
W1-ALE	3.78 ± 0.40	0.07 ± 0.02	3.31 ± 0.43	0.921
W2-ALE	4.05 ± 0.22	0.10 ± 0.03	1.27 ± 1.79	0.965

transfer of certain strains over others) and natural/artificial selection (Justice et al., 2017). Moreover, coexisting species in microbial communities can evolve over time by random mutations, which alter the interactions between species leading to the shifts in their composition (McEnany and Good, 2024). It is often observed that microbial consortia with different compositions and different enzyme activity profiles show overall similar functionalities, due to functional redundancy across (and within) the microbial communities (Cortes-Tolalpa et al., 2016; Wongwilaiwalin et al., 2013). The two enriched consortia (W1 and W2) in this study showed different relative abundances but were predicted to have

overlap functionalities using PICRUSt2 tool (Fig. S2). Therefore, for the benefit of overall bioprocesses efficiency, it is important to focus on adaptive evolution of microbial communities that leads to the selection of improved phenotypes and functionalities (communities with enhanced functions of interest) (Dragosits and Mattanovich, 2013; Lalejini et al., 2022), rather than a certain microbial composition. It was previously reported that properly enriched and stable functional consortia can be considered as a “superorganism”, which can act in a stable/reproducible way, (from a metabolic and functional point of view), thus allowing to use predictive modelling and statistical optimization (Varrone et al., 2018).

3.3. Adaptive laboratory evolution of enriched consortia on PO pyrolysis wax

W1 and W2 were sub-cultured during their exponential growth phase in MSM, with a stepwise increase in PO wax concentration from 1% to 6% (w/v). Subcultures were grown at a specific substrate concentration for several transfers, until reaching a stable maximum OD. We observed that the higher the concentration of PO wax, the longer the lag phase of both consortia. Thus, the time of incubation before each transfer varied from 1 to 3 d, to allow reaching the exponential growth phase. Increasing PO wax concentration to more than 4% (w/v) did not further

improve OD600 after 3 d of incubation (Fig. S3). ALE was stopped after increasing the concentration to 6%, also due to challenges in keeping a stable emulsion. The growth curves of the evolved consortia (hereafter, W1-ALE and W2-ALE) were compared with the original enriched consortia (consortium W1 and W2) before ALE (Fig. 3). Stationary phase was reached within 3 d, and the maximum OD600 was approximately 4.0 for both W1-ALE and W2-ALE, showing a clear improvement from the enriched consortia W1 and W2 (4- and 3.1-fold improvement in OD600, respectively) (Table 1). The growth rate of ALE consortia also increased by 1.8 and 10.0 times, respectively. W2-ALE had a slightly higher growth rate, as well as a 2.6 times shorter lag phase. The lag phase of W2 was 22.5 h and was dramatically shortened to 1.3 h after ALE, even though it was not significantly changed in the case of W1. This result suggests that ALE can serve as an effective strategy for the adaptation of bacterial consortia to utilize better the PO pyrolysis wax, improving growth rate and biomass yield, despite a certain biological variability.

3.4. PO wax emulsion preparation with two monomeric surfactants

PO wax emulsion was initially prepared in MSM by ultrasonication at the intensity of 60%. However, instability of the emulsion was observed (Fig. S4); thus, a new emulsification method was designed by modifying the protocol from the previous work by Mir and Ghasemirad (2022). Mineral oil was added to create a blend with PO wax. As previously mentioned, increasing the oil ratio in paraffin oil/PO wax blend helps decreasing the drop size of oil-in-water emulsion. Three water-soluble surfactants, including Tween 20, Tween 80, and Tween 85, were screened for their ability to promote PO wax bioconversion compared to the process without surfactant (Fig. S5). Tween 20 was found to be the best water-soluble surfactant to promote cell biomass accumulation; thus, it was selected for the use in the two monomeric surfactants process. Two monomeric surfactants, water-soluble Tween 20 and oil-soluble Span 80, were used as emulsifiers to reduce the coalescence of emulsion droplets and eventual phase separation. Span 80-paraffin oil/PO wax blend and Tween 20-water solution were vigorously mixed, and the dispersion of oil/wax droplets in water were enhanced by ultrasonication at higher intensity (80%). This approach allowed to enhance the stability of the emulsion (Fig. S4) and the proper consumption of PO wax by microbes. However, a small amount of flocculation of emulsion particles at the top of the aqueous phase was still observed. This could be caused by the presence of ions in MSM and/or the growth of microbes. The presence of divalent ions in the aqueous phase was reported to influence the crude oil emulsion stability (Parajuli

et al., 2020). The same study also reported that incubation of crude oil emulsion with bacteria led to the emulsions breaking within 5 d at the temperature of 32 °C and shaking at 120 rpm. The stability of the micelles might be destroyed because the microbes also degrade the surfactants, releasing the hydrocarbons present in the micellar core which then migrate to a different phase with water (Mohanty et al., 2013). It is therefore essential to select microorganisms with a high affinity for the wax that can rapidly (<5 d) convert the substrate. The enrichment of surfactant producers (such as *Achromobacter*) can be a further advantage to counteract eventual surfactant biodegradation.

3.5. Microbial conversion of PO pyrolysis wax in bioreactor scale

Microbial conversion was performed in batch with 10 g L⁻¹ initial PO pyrolysis wax emulsified in MSM with two surfactants, as described earlier. Consortium W2-ALE was used as inoculum, due to its higher growth rate on PO wax. The process was controlled at pH 7.0, 30 °C, with a partial oxygen pressure of 20%. The growth data was collected over a period of 48 h. Bioreactor cultivation promoted a higher growth rate of microbial consortia, entering the stationary phase within 24 h (3 times faster than shake flask cultivation), probably due to better control of the oxygen transfer rate and mixing of the substrate. The OD600 after 48 h cultivation was 5.7, corresponding to 2.95 g L⁻¹ of CDW. OD600 and CDW trends are shown in Fig. 4a. It should be noted that the emulsification method used in this experiment included the addition of mineral oil, Tween 20, and Span 80. Therefore, the growth of microbial consortia on mineral oil (1% w/v) as the carbon source (using the same emulsification method) was performed as a negative control, showing an OD600 in 48 h of 2.5 (corresponding to 1.41 g_{CDW} L⁻¹), indicating that the biomass growth in this experiment was obtained from both PO wax and mineral oil. Subtracting the growth data with the negative control, cell biomass of 1.54 g_{CDW} L⁻¹ was obtained from PO wax substrate in 48 h-cultivation, which is comparable with what can be observed in shake flask cultivation in 5 d (1.45 g_{CDW} L⁻¹). This result shows 60% faster cell biomass productivity with bioreactor cultivation.

Fig. 4b shows the substrate consumption over time during microbial conversion. Notably, 87.3% of PO wax was consumed within 12 h of cultivation and 100% consumption was observed within 48 h, corresponding to a yield of 0.3 g_{Biomass} g_{PO wax}⁻¹. Alkanes with a chain length longer than C9 (found in the PO wax used in this study) generally do not inhibit the growth of microbes, due to their hydrophobicity and low bioavailability (Singh et al., 2012). However, the uptake mechanisms for different chain lengths vary by species and could be limited at high concentration (Fenibo et al., 2023). A previous study showed that the

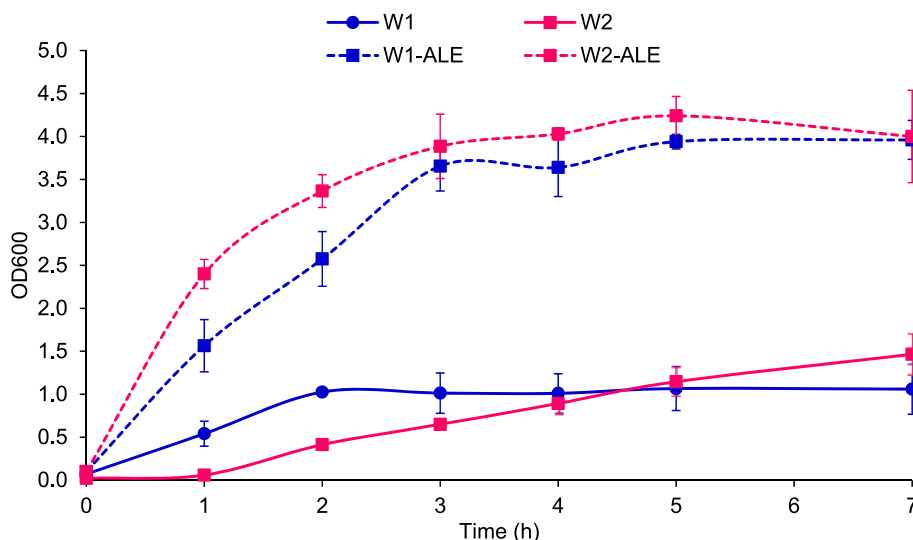


Fig. 3. Growth curves of W1 and W2 before and after ALE.

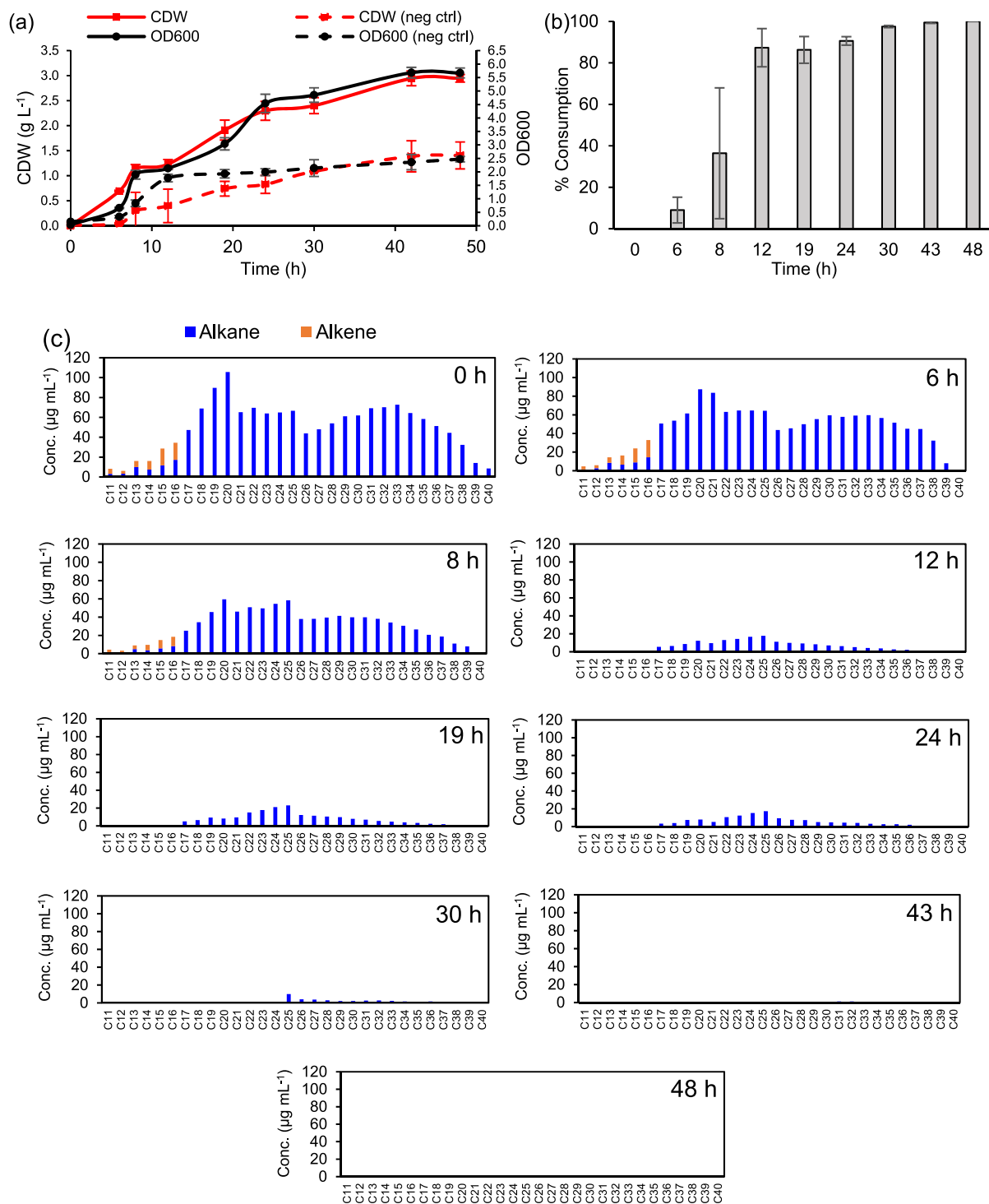


Fig. 4. Growth characteristics of microbial consortium W2-ALE (a), and substrate consumption percentage (b) and profile (c) during the bioconversion process of PO pyrolysis wax (10 g L⁻¹) in 2 L-bioreactor controlled at pH of 7.0 and pO₂ of 20% (a) (reported data showing only PO wax, not including mineral oil).

uptake of octadecane at a concentration lower than 1.15 mg L⁻¹ occurred by ATP-driven *trans*-membrane transport (active transport), while the higher concentration was facilitated by the passive transport, following the intra/extra substrate concentration gradient in *Pseudomonas* sp. (Hua et al., 2013). Similar mechanisms could be expected from the bacteria in the same class of γ -Proteobacteria like *Stenotrophomonas* sp. (the dominant genus found in enriched consortium W2 in this study).

Hydrocarbon-degrading microorganisms are equipped with enzymes

that convert different chain-length of hydrocarbons, such as methane monooxygenase (C1-C4), alkane monooxygenases (C5-C16), cytochrome P450 monooxygenases (C5-C16), dioxygenases (C10-C30) (Abbasian et al., 2015). As a few examples, *Alcanivorax borkumensis* has genes coding for three cytochrome P450s and two integral membrane alkane hydroxylases (AlkB1 and AlkB2, which have substrate specificity for C5-C12 and C8-C16, respectively) (Miri et al., 2010). *Geobacillus* species, identified to have alkane monooxygenase gene LadA, can utilize long-chain alkanes (C15-C36) via a terminal oxidation pathway (Feng

et al., 2007). *Acinetobacter oleivorans* and *Acinetobacter baylyi*, equipped with LadA and flavin adenine dinucleotide-dependent single-component flavoprotein (AlmA), were shown to degrade a range of alkanes from C12-C30, and so does *Stenotrophomonas pavanii* and *Pseudomonas aeruginosa* (Bhattacharya et al., 2020; Liu et al., 2014; Park et al., 2017; Yin et al., 2024). *Stenotrophomonas* sp. was reported before to have the conserved chromosomal region encoding AlkB-Rubredoxin (RubA) fused proteins which extend the spectrum of alkane degradation to more than C16 (up to C36) (Venkidusamy and Megharaj, 2016). Rubredoxin-type Fe(Cys)₄ protein, an essential electron transfer component for alkane hydroxylation, was also found present in *Sphingobacterium* sp. (Shapiro et al., 2022), which was the second most abundant genus in enriched W2 consortium in this study.

Fig. 4b shows that more than 80% of alkanes of all chain lengths were consumed within 12 h. Alkanes with carbon length from C11-C16 were completely consumed within 30 h (or 3.3% consumption h⁻¹), while those with carbon length from C17-C40 were consumed at a slower rate (complete consumption in 48 h, or 2.1% consumption h⁻¹) (Fig. 4c). This could be explained by the presence of bacterial genera reported to be equipped with AlkB that prefer C ≤ 16 alkanes in W2-ALE consortium (*Stenotrophomonas*, *Sphingobacterium*, *Achromobacter*, *Acinetobacter*, and *Pseudomonas*). While the dominant genus *Stenotrophomonas* and other genera like *Acinetobacter* and *Pseudomonas* were reported to also be able to degrade C ≥ 16 alkanes. Thus, the consumption of all chain lengths found in the PO wax was observed. Complementary enzyme machinery in MMCs can potentially promote the use of hydrocarbon mixtures, as has been seen before in the biodegradation of crude oil (Chen et al., 2014; Wu et al., 2023; Zhang et al., 2021). Alkenes from C11-C16 were also found in the PO wax, with 4% and 37% consumed in 6 and 8 h, respectively. Complete consumption of alkenes was observed within 12 h.

More than 80% of PO wax was consumed in 12 h in this study, which is 4 times faster than what was previously reported, where a similar consumption of PE wax was reached within 48 h by *P. aeruginosa* GL-1 in a shake flask experiment (Guzik et al., 2014). Another study using oil from hydrothermally processed PE (which had a similar composition to PE wax but was mainly composed of C8-C13) as the carbon source for the fermentation process by *Yarrowia lipolytica* showed 67% substrate consumption in 72 h (Torres-Zapata et al., 2022). As shown in the current study, employing an enriched and adapted MMC allows the complete utilization of hydrocarbons from C11-C40 at a faster rate than what has been reported with monocultures.

Enriched MMCs were also developed to use PE deconstruction products obtained by catalytic hydrogenolysis, by Gregory and colleagues, showing 85–86% consumption of alkanes in 14 d (Gregory et al., 2023). The improved substrate consumption rate in our study could be due to 1) the prolonged enrichment followed by ALE with a stepwise increase of substrate concentration (from 1% to 6%) and 2) the enhanced accessibility of PO wax by preparing an improved emulsion. In fact, efficient emulsification of PO wax with surfactants can pseudo-solubilize hydrocarbon components by producing micro-droplets in the biosurfactant micelles (Hua and Wang, 2014), enhancing the uptake of PO wax, without the need for a high-cost oxidation step. However, a possible boosting effect of the mineral oil co-metabolism cannot be ruled out. Nonetheless, the PO wax consumption rate in this study was 1.2–35 times higher than what was previously reported with similar substrates (Table S1).

Moreover, in this study, we used the PO wax concentration of 10 g L⁻¹ in the bioreactor-scale process, which is higher than most of the previous reports and similar to the process using PE oil studied by Torres-Zapata et al. (2022). However, the microbial consortia W2-ALE was able to grow in 60 g L⁻¹ PO wax in shake-flask experiment, with the maximum OD₆₀₀ of 9.9 (CDW of 5.2 g L⁻¹) (Fig. S3), even though poor stability of PO wax emulsion was observed, leading to the aggregation of PO wax into big lumps that were inaccessible to microbes and caused low biomass yield (0.09 g_{Biomass} g_{PO wax}⁻¹).

3.6. Analysis of products from bioconversion process

PO pyrolysis wax is composed of a mixture of hydrocarbons which are highly reduced molecules with high energy and carbon content, serving both as carbon and energy sources for microorganisms. Aerobic degradation of linear hydrocarbons typically starts with the initial enzymatic oxidation on the different positions of the carbon atom: terminal, biterminal, subterminal, and the Finnerty pathway. In terminal and subterminal oxidation pathways, alkane hydroxylase is the first enzyme to hydroxylate the alkane molecules at the terminal methyl group or subterminal methylene position (Ji et al., 2013; Liu et al., 2014; Rojo, 2010; Van Beilen and Funhoff, 2007). Primary or secondary alcohols generated from the oxidation pathways are subsequently converted to aldehydes and fatty acids by alcohol dehydrogenase and aldehyde dehydrogenase, respectively, and are then further metabolized via β-oxidation, resulting in the production of biomass and CO₂ (Abbasian et al., 2015; Ji et al., 2013). Fatty acids can also be assimilated into microbial cells as a component of the cell membrane, or converted to intracellular molecules such as triglycerides, wax esters, or PHAs under specific imbalanced growth conditions like an excessive carbon-to-nitrogen ratio (Alvarez, 2003).

To identify the potential valuable products from the PO pyrolysis wax bioconversion process, extracellular products were first investigated by GC-MS analysis of dichloromethane extracted supernatant. The identification by NIST library showed the mixture of branch-chain alkanes, alcohols, acids, and possibly secondary microbial metabolites in the extracted supernatant (Table S2). However, relative low intensity of product peaks compared to substrate peaks led to poor identification accuracy, and possibly means low titer of products. Therefore, intracellular metabolites were investigated instead. Fatty acid profiles of triglycerides accumulated in biomass grown on PO pyrolysis wax in bioreactor-scale cultivation were analyzed by GC-FID as fatty acid methyl esters (FAMES), after transesterification. The total fatty acids concentrations increased through cultivation time and reached the maximum at 30 h (105.5 mg L_{reactor}⁻¹) and declined at 48 h (86.3 mg L_{reactor}⁻¹) (Fig. 5a). The yields of total FAMES per cell dry weight decreased from 37.1 mg_{FAMES} g_{CDW}⁻¹ at 6 h to 25.1 mg_{FAMES} g_{CDW}⁻¹ at 24 h, but significantly increased again and reached the maximum at 30 h (43.9 mg_{FAMES} g_{CDW}⁻¹).

The changes in fatty acid compositions are shown in Fig. 5b. Both saturated and unsaturated fatty acids were detected in the biomass samples. Seven even-numbered saturated fatty acids from C14-20 were found, with methyl palmitate (C16:0) as the main component in total fatty acids analyzed at every time point (39–46%). Five different species of unsaturated fatty acids (C14:1, C15:1, C16:1, C18:1 (*cis*- and *trans*-), and C20:1) were also detected. Saturated fatty acids content increased over time and reached the maximum of 86.6% at 42 h, meanwhile, unsaturated fatty acids decreased proportionally. High content of methyl *trans*-9 elaidate (C18:1) (25–26%) was found during 6–12 h but decreased afterward and was substituted by the higher content of methyl arachidate (C20:0) during 30–48 h (24–35%). The composition of fatty acids might be affected by both substrate and bacterial composition in the microbial mixed consortia. PO pyrolysis wax used in this work has saturated hydrocarbon as the main composition, which might contribute to the higher proportion of saturated fatty acids. A previous study reported a significantly higher C16:0 content from fuel oil-degrading *Stenotrophomonas maltophilia*, when saponin and Triton X-100 were used as surfactants, compared to their negative control (no fuel oil added), while C15:0 *anteiso* and C17:0 *anteiso* contents were more abundant when rhamnolipid was used (Kaczorek et al., 2013). A bacterial consortium composed of *Bacillus* spp. and *Pseudomonas putida* grown on cooked butter waste and olive oil was reported to have C16:0, C16:1, and C18:1 as the main compositions of intracellular fatty acids (Tziritza et al., 2018), underlining the effect of the feedstock composition on the fatty acid spectrum.

The maximum total fatty acids concentration found in the current

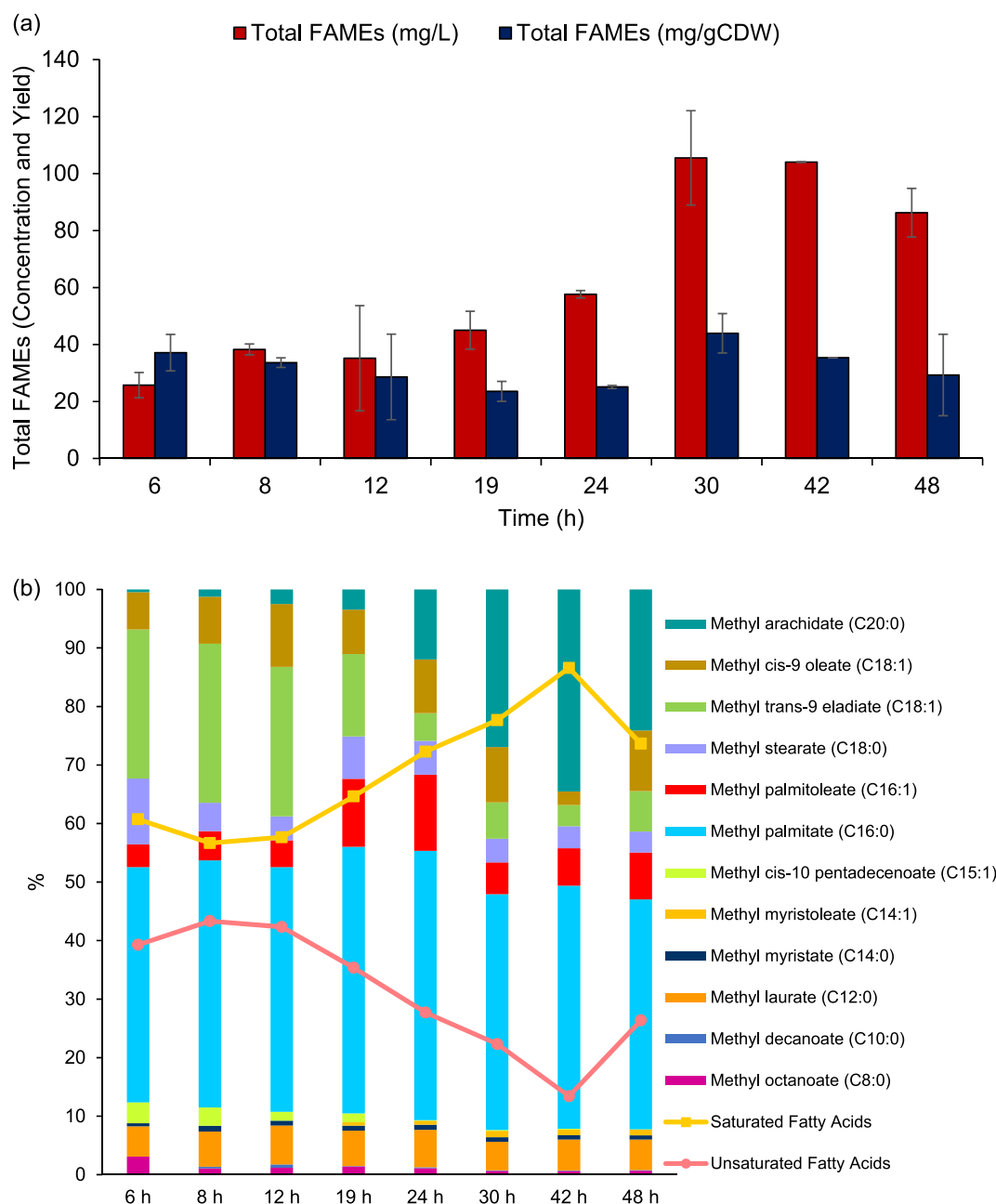


Fig. 5. Total FAMES concentration and yield (a) and FAMES profile (b) analyzed from W2-ALE biomass grown on PO pyrolysis wax.

study was $105.5 \text{ mg}_{\text{FAMES}} \text{ L}^{-1}$ at 30 h bioconversion, which was 4.5 times higher than previously reported using 15 g L^{-1} PE oil from hydrothermal processing to grow *Y. lipolytica* for 72 h (Torres-Zapata et al., 2022). The same study mentioned that *Y. lipolytica* was not able to grow on viscous yellowish wax formed at $425 \text{ }^{\circ}\text{C}/60 \text{ min}$ hydrothermal treatment of PE (which is similar to the substrate used in this study). This indicates that the adapted microbial consortia have higher robustness toward such inhibiting and complex substrates than the pure strain. Five times higher total fatty acids production (526.3 mg L^{-1}) was reported by growing *Y. lipolytica* on 15 g L^{-1} pyrolyzed PP oil -emulsified media after 120 h-cultivation (Mihreteab et al., 2019). Such oil was composed of 50.9% branched fatty alcohols, 25.1% branched alkenes, 10.4% cyclic alkanes, 9.5% branched alkanes, 1.4% thiols, 1.1% ketones, and others. Since the major compositions of this substrate were oxidized compounds (alcohols and ketones), as well as the formulation of their media with 4.5 g L^{-1} oleic acid as an added emulsifier, this could be the reason for the enhanced fatty acids accumulation. Oleic acid was the major fatty

acid from the process, followed by palmitoleic, palmitic, stearic, and arachidic acid, respectively. A nearly four-fold increase in fatty acids titer was reported when the media optimization was performed (change of nitrogen source from $(\text{NH}_4)_2\text{SO}_4$ to Yeast Nitrogen Base, using 2.5 g L^{-1} yeast extract) (Mihreteab et al., 2021). It is important to highlight that liquid oil from pyrolysis of polyolefins can be refined for fuel-like applications, while the wax fraction is normally used in downcycling application like a coating material or a blend for road construction materials (Abdy et al., 2022; Krupa et al., 2007). Therefore, the bio-upcycling process developed on the wax fraction might be an important strategy to avoid downcycling.

From a waste management and recycling perspective, the complete mineralization of PO pyrolyzed products to CO_2 would lead to a material loss from the plastic value chain and should be avoided by channeling the carbon flux toward recoverable materials, such as intracellular storage polymers. One of the high value intracellular products are PHAs. They are biodegradable and biocompatible polymers with a wide range

of applications, expected to share 13.5% of the bioplastic market in 2028 (European Bioplastics, 2023). PHAs are accumulated in microbial cells under stress and imbalanced growth conditions, such as the depletion of nitrogen, phosphorus, or oxygen sources in the presence of high carbon concentrations (Behera et al., 2022). A nitrogen limitation strategy was shown to successfully upcycle thermo-chemically treated PE into PHA, for instance by cultivating *P. aeruginosa* GL-1 on 20 g L⁻¹ PE pyrolysis wax in nitrogen-limiting MSM (0.25 g L⁻¹ NH₄Cl or 0.065 g N L⁻¹) for 48 h, reaching 0.39 g_{CDW} L⁻¹ and 18.9% PHA (Guzik et al., 2014).

In the current study, we identified several strains from the enriched and adapted W1 and W2 consortia that are reported to produce PHAs. In particular, *Stenotrophomonas*, *Achromobacter*, *Alcaligenes*, *Pseudomonas*, and *Ochrobactrum* have been reported to produce poly(3-hydroxybutyrate) (PHB) (Clifton-García et al., 2020; Mahendhran et al., 2018; Sayyed et al., 2021; Venkateswar Reddy et al., 2017). *Pseudomonas* and *Sphingobacterium* have also been reported to produce mcl-PHAs (Bustamante et al., 2019; Davis et al., 2013; Tamboli et al., 2010). This suggests a potential for rapid upcycling of PO wax into PHAs.

However, the cell biomass from bioreactor cultivation in this study accumulated very low amount of PHA (1.3–2.0% PHA per CDW), probably due to high nitrogen concentration in the culture media (2 g L⁻¹ (NH₄)₂SO₄). Thus, process optimization was performed to investigate the potential of bioupcycling PO wax into PHAs.

3.7. Statistical optimization of PHA production from PO wax using the MMC bioconversion process

Nitrogen-limiting condition (0.065 g N L⁻¹) was applied to induce PHA accumulation in the MMC bioconversion process. Inorganic nitrogen sources, including NH₄Cl, (NH₄)₂SO₄, NaNO₃, and NaNO₂, were first compared for their effect on PHA production using PO wax (10 g L⁻¹) as a sole carbon source. CDW was not significantly different among all nitrogen sources tested; however, NaNO₃ promoted the highest PHA accumulation at 14.8% per CDW (Fig. S6). This suggests that the adapted MMC developed in this study has the potential to be used for bioupcycling PO wax to PHA. Thus, statistical optimization was performed to further improve PHA accumulation and titer. NaNO₃ was chosen as a nitrogen source. C/N was used as one of the design variables instead of nitrogen concentration based on the preliminary data showing that C/N is more likely to affect PHA accumulation by this MMC. PO wax concentrations from 1 to 40 g L⁻¹ were preliminary screened to decide the range in the Design of Experiment, and (as discussed before) the

instability of PO wax emulsion was observed at the concentration higher than 20 g L⁻¹, associated with no improvement in PHA production (Fig. S7). Thus, the PO wax concentration from 1 to 20 g L⁻¹ was used.

Three parameters were observed for their interactive effect on PHA production by MMC, including PO wax concentration (A), C/N ratio (B), and inoculum size (C). Multiple regression was used to analyze the responses, namely PHA titer and %PHA per CDW, by fitting quadratic polynomial models. The main results of experimental runs are reported in Table 2 as the average of three replicates for each condition. Inverse square root and natural log were applied as the data pretreatment to experimental PHA titer and %PHA per CDW, respectively. The coefficient of determination (R²) for the quadratic model with the best fit for PHA titer (Eq. (1)) and %PHA (Eq. (2)) was 0.8942 and 0.9201, thus explaining more than 89% and 92% of their total variability, respectively. Adjusted R² and predicted R² are in reasonable agreement, and the values are higher than 0.8, which is considered a good fit of generated models to the experimental data. The adequate precisions for the quadratic model fitted for PHA titer and %PHA were 21.5523 and 22.6726, respectively, indicating a sufficient signal-to-noise ratio (>4). Both models had p-values less than 0.05, which is considered statistically significant. All design variables significantly affected PHA titer (p-value <0.05), but only PO wax concentration and C/N ratio affected %PHA. The complete ANOVA and fit statistics were reported in Table S3.

$$[\text{Sqrt}(\text{PHA titer})]^{-1} = 0.0954 - 0.0335A - 0.0149B - 0.0157C - 0.0006AB + 0.0038AC + 0.0025BC + 0.0097A^2 + 0.0302B^2 + 0.0086C^2 \quad (\text{Eq. 1})$$

$$\ln(\% \text{PHA}) = 2.23 - 0.2543A + 0.6861B + 0.0365C - 0.2743AB - 0.0244AC - 0.0453BC + 0.6116A^2 - 0.5419B^2 - 0.1925C^2 \quad (\text{Eq. 2})$$

3D surface plots showed that higher PO wax concentration would result in higher PHA titer, while the opposite was observed for %PHA (Fig. 6). Notably, PHA titer is affected by both %PHA and CDW; thus, higher carbon concentrations that promote higher cell biomass production can lead to higher PHA titer even with the lower %PHA. The best PHA titer from the conducted experiments was 225.5 mg L⁻¹ from the run with a PO wax concentration of 20 g L⁻¹, C/N ratio of 52.5, and inoculum size of 10.5%. MMC cultured with this condition accumulated PHA at 13.3%. However, the maximum PHA per CDW observed was 31.1% with a PO wax concentration of 1 g L⁻¹, C/N ratio of 100, and inoculum size of 1%. This is coherent with previous findings that showed how lower inoculum size could lead to a higher %PHA accumulation (Khamkong et al., 2022; Sindhu et al., 2011). Internal growth limitation could be another condition that enhances PHA synthesis, besides

Table 2

Experimental data of PHA production from PO wax by MMC (W2-ALE) and comparison of predicted values from generated model and observed values after applying the optimal process parameters for PHA production in MMC (W2-ALE) bioconversion process. The shown data of each condition is the average of its replicates (AVG ± SD).

[PO wax] (g L ⁻¹)	C/N	% inoculum	CDW (g L ⁻¹)	% PHA per CDW	PHA titer (mg L ⁻¹)	PHA yield (mgPHA gPO wax ⁻¹)
1	5	1	0.70 ± 0.01	3.28 ± 0.81	22.91 ± 5.32	22.91 ± 5.32
1	5	20	0.76 ± 0.04	4.20 ± 0.11	31.93 ± 2.03	31.93 ± 2.03
1	52.5	10.5	0.20 ± 0.01	25.04 ± 2.62	50.81 ± 3.98	50.81 ± 3.98
1	100	1	0.09 ± 0.01	31.09 ± 3.74	28.77 ± 2.11	28.77 ± 2.11
1	100	20	0.21 ± 0.02	27.43 ± 2.16	56.89 ± 8.51	56.89 ± 8.51
10.5	5	10.5	1.65 ± 0.36	3.88 ± 0.35	63.94 ± 12.79	6.09 ± 1.22
10.5	52.5	1	1.17 ± 0.02	7.09 ± 1.26	82.86 ± 5.45	7.89 ± 0.52
10.5	52.5	10.5	1.28 ± 0.05	8.71 ± 2.35	111.50 ± 30.35	10.62 ± 2.89
10.5	52.5	20	1.17 ± 0.07	9.31 ± 0.53	109.08 ± 11.15	10.39 ± 1.06
10.5	100	10.5	0.79 ± 0.03	8.64 ± 2.12	68.05 ± 15.77	6.48 ± 1.50
20	5	1	1.06 ± 0.06	4.04 ± 0.38	42.97 ± 6.14	2.15 ± 0.31
20	5	20	2.35 ± 0.56	3.88 ± 0.28	92.28 ± 27.77	4.61 ± 1.39
20	52.5	10.5	1.69 ± 0.12	13.27 ± 1.97	225.47 ± 48.30	11.27 ± 2.41
20	100	1	1.01 ± 0.02	10.52 ± 0.40	106.62 ± 5.09	5.33 ± 0.25
20	100	20	1.27 ± 0.12	10.61 ± 2.61	135.19 ± 40.70	6.76 ± 2.04
20	63.37	16.77	1.81 ± 0.20	21.26 ± 0.21	384.09 ± 46.48	19.20 ± 2.32
					(Model prediction: 264.04 mg/L)	
1	94.52	11.01	0.16 ± 0.02	34.76 ± 1.43	56.16 ± 8.47	56.16 ± 8.47
				(Model prediction: 34.87 %)		

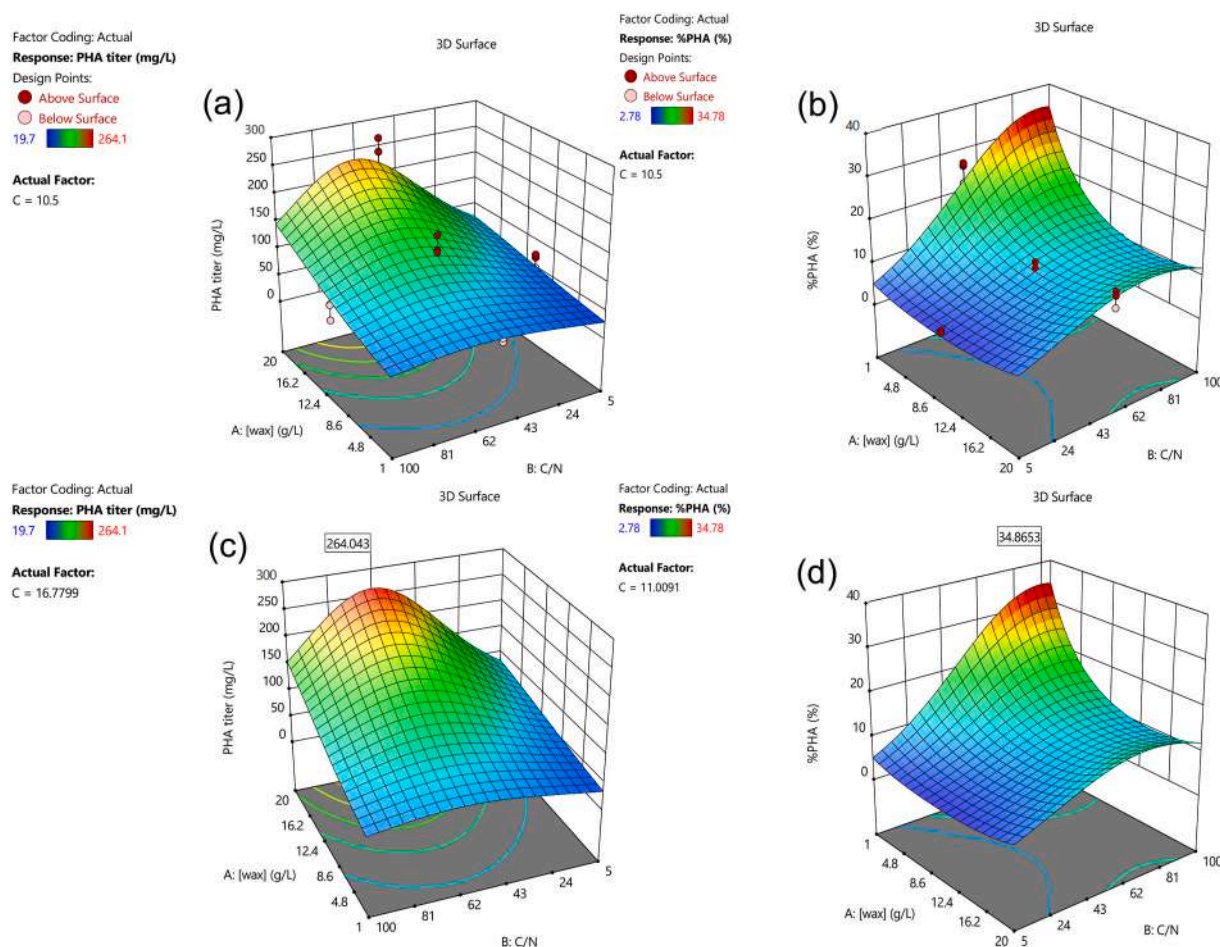


Fig. 6. 3D surface plot of the Response Surface Quadratic Model for experimental PHA titer at the inoculum size of 10.5% (a) and %PHA per CDW (b), and the optimization of process parameters to maximize PHA titer (c) and %PHA per CDW (d) from MMC (W2-ALE) bioconversion process.

external growth limitations like lack of nutrients (Albuquerque et al., 2010). Therefore, a slow growth rate due to low starting inoculum might cause insufficient intracellular components and induce PHA storage (Serafim et al., 2008). Nevertheless, it also depends on the type and concentration of substrate. Higher inoculum size can be necessary to overcome the inhibitory effects of high concentrations of toxic or inhibiting substrates (Mahato et al., 2023).

The model predicted a maximum PHA titer of 264.0 mg L^{-1} using the condition with PO wax concentration of 20 g L^{-1} , C/N of 63.4, and inoculum size of 16.8%. Model validation was performed by PHA production in batch cultivation using the optimized condition. The experimental PHA titer was 384.1 mg L^{-1} , which significantly deviated from the predicted value (Table 2). This discrepancy might be attributed to the significant Lack of Fit of such model (Table S3). A possible reason could be that the face-centered CCD was used as a DoE for generating the model in this study. Normally, rotational CCD would give the model with better quality of prediction and no bias, as the axial points established the extreme low and high values from the faces of design cube (Sarwar and Rahman, 2021). However, rotational CCD designed the experiment to have axial points with a distance from the center (α) of 6.477; thus, the suggested range of $(-\alpha, +\alpha)$ would be $(-5.477, 26.477)$, $(-27.385, 132.385)$, and $(-5.477, 26.477)$ for PO wax concentration, C/N, and inoculum size, respectively. As the negative values of such parameters (e.g., PO wax concentration of -5.477 g L^{-1}) cannot be experimentally performed, we selected face-centered CCD design ($\alpha = 1$) which gave the $(-\alpha, +\alpha)$ of (1, 20), (5, 100), and (1, 20) for PO wax concentration, C/N, and inoculum size, respectively. The responses beyond the defined variable bounds will be in the design region when

using rotational CCD but only be extrapolated with face-centered CCD which could cause the lower quality of prediction. Nevertheless, the model generated from the face-centered CCD can also precisely predict the responses. The model generated for %PHA gave accurate prediction, with an accumulation of 34.9% PHA, using the condition with PO wax concentration of 1 g L^{-1} , C/N of 94.5, and inoculum size of 11.0%. The experimental value was 34.8% (0.3% deviation), confirming the validity of this model. The precision of the model may also depend on the type of responses; for instance, the PHA titer is the combination of two responses, cell biomass concentration and %PHA, which could be more sensitive and thus exhibit higher deviation.

The optimized condition for maximizing PHA titer allowed 5.6 times improvement from the initial titer (68.1 mg L^{-1}) using nitrogen-limiting media (0.065 gN L^{-1}). On the other hand, %PHA obtained in this condition was 21.3%, which was somewhat higher than observed before optimization (14.8%). However, the maximum %PHA achieved in this study was 34.8% (2.4 times higher than what was initially observed) when using low PO wax concentration (1 g L^{-1}) and high C/N (94.5). While this high C/N ratio promote more PHA accumulation, the total cell biomass was very low ($0.16 \text{ g}_{\text{CDW}} \text{ L}^{-1}$), thus resulting in low PHA titer. So, despite the promising results by the statistical optimization, higher titers need to be obtained for a scalable and more economically viable PHA production processes. Clearly, as PHAs are an intracellular product associated with cell growth, both %PHA and cell biomass production must be maximized to get a higher final titer. While batch tests are a good choice for statistical optimization (thanks to a good control and the possibility of having numerous and independent replicates, etc.), other options should be considered to maximize both, cell growth

and accumulation of PHAs. After all, high concentrations of carbon source cannot be applied when working with complex and inhibiting substrates such as PO wax. This suggests that other feeding strategies than batch should be tested as well. Recent studies seem to confirm that PHA process can be further improved by using fed-batch cultivation in which the maximum production of cell biomass is performed before applying a nitrogen-limiting condition, to enhance PHA accumulation with different feeding strategies, e.g., pulse feeding, exponential feeding, or hybrid feeding (Guzik et al., 2022; Nygaard et al., 2023).

The composition of the PHA should be also considered, to assess and eventually tune the processability and mechanical properties required, based on the expected applications. In the current study, the PHA monomer distribution analysis showed that scl- and mcl-PHA was produced by the adapted MMC, which was expected from the variety of microbial composition of the consortium. 3-hydroxyalkanoic acids from C4 to C12 were observed. More in detail, C8 (16%), C9 (20%), and C10 (30%) were the dominant monomers when using the condition that maximized PHA titer. The monomer distribution changed when using the condition to maximize %PHA with C8 (46%) and C10 (27%) becoming dominant, possibly due to microbial proportion fluctuation in MMC, forced by the different culture conditions (Fig. S8). mcl-PHAs are highly elastomeric, making them ideal for medical applications such as soft tissue engineering (Hahn et al., 2024) and adhesives for wound closure or wound dressings (Pereira et al., 2019), showing great potential to upcycle PO waste to the high-value PHAs.

4. Conclusions

This study developed the bioconversion process to upcycling the PO wax (side stream from PO pyrolysis process that has low value), to complement the PO recycling process. The obtained PO wax was made of C11-C40 hydrocarbons in solid form, which are inaccessible by microorganisms. We applied a modified emulsification method by using mixed emulsifiers, including water-soluble surfactant (Tween 20) and oil-soluble surfactant (Span 80), to produce a PO wax emulsion with the good stability (up to 20 g L⁻¹) in microbial growth medium. Functional MMC were developed through enrichment on PO wax followed by ALE, which increased 4 times cell biomass and led to 2.6–17.3 times shorter lag phase. The consortium W2-ALE showed complete bioconversion of PO wax in 48 h in bioreactor-scale cultivation, yielding 0.3 g_{Biomass} g_{PO wax}⁻¹. Extracellular products were not fully identified, but a good production of cell biomass (2.95 g_{CDW} L⁻¹) was observed, as expected from such a highly reduced substrate. Intracellular products such as triglycerides, comprised both saturated and unsaturated from C14-C20, were observed (105.5 mg_{FAMES} L⁻¹) and represent a possible strategy for the valorization of PO waste into higher-value compounds. W2-ALE also showed the capability to accumulate mcl-PHA (mainly composed of C8, C9, and C10 monomers); thus, the process condition was statistically optimized to enhance PHA production. Such process would allow to biopcycle fossil-derived plastic waste into bioplastics. Maximum PHA titer reached 384.1 mg L⁻¹ (with 1.81 g_{CDW} L⁻¹ and 21.3% PHA per CDW) using the PO wax concentration of 20 g L⁻¹, C/N ratio of 63.4, and inoculum size of 16.8%. Enhanced %PHA accumulation was possible by using lower PO wax concentration (1 g L⁻¹) and higher C/N ratio (94.5), reaching almost 35% PHA per CDW. However, the low nitrogen concentration limited the growth of the MMC, showing a low amount of total biomass (0.16 g L⁻¹), thus resulting in low PHA titer. Future work should focus on designing the fed-batch process to firstly increase cell biomass accumulation and later induce PHA accumulation to achieve high titers and decrease downstream processing costs.

In conclusion, this study proposes an integrated process to upcycle non-biodegradable PO by using PO wax from a commercial pyrolysis process and microbial bioconversion to triglycerides and PHAs. Enriching plastic landfill-derived microbial communities on PO pyrolysis wax allowed to select robust microbial communities able to grow on the substrate, while ALE boosted substrate consumption efficiency and

tolerance. The bioconversion process was developed in shake flasks and then transferred in a bioreactor, which improved microbial growth rate. This study represents a first step towards the upcycling of recalcitrant substrates such as unrecyclable plastic waste streams, potentially contributing to the increased circularity of the future plastic sector.

CRedit authorship contribution statement

Passanun Lomwongsopon: Methodology, Validation, Formal analysis, Investigation, Data Curation, Writing – Original Draft, Writing – Review & Editing, Visualization. **Tanja Narancic:** Methodology, Writing – Review & Editing. **Reinhard Wimmer:** Methodology, Formal analysis, Writing – Review & Editing. **Cristiano Varrone:** Conceptualization, Methodology, Resources, Writing – review & editing, Supervision, Project administration, Funding acquisition.

Declaration of competing interest

The authors declare no competing interests.

Acknowledgements

This work was supported by the H2020 UPLIFT project [Grant Agreement no. 953073]. The authors wish to thank WPU and Anders Egede Daugaard from Technical University of Denmark for the supply of PO wax. The authors are also thankful to Simon Gregersen Echers for helping with GC-MS and all BioCat Lab members at University College Dublin, especially Manuel Bruch, Karthika Balusamy, and Meg Welsh, for technical support and laboratory help.

Appendix A. Supplementary data

Supplementary data to this article can be found online at <https://doi.org/10.1016/j.chemosphere.2024.143671>.

Data availability

Data will be made available on request.

References

- Abbasian, F., Lockington, R., Mallavarapu, M., Naidu, R., 2015. A comprehensive review of aliphatic hydrocarbon biodegradation by bacteria. *Appl. Biochem. Biotechnol.* 176, 670–699. <https://doi.org/10.1007/S12010-015-1603-5>.
- Abdy, C., Zhang, Y., Wang, J., Yang, Y., Artamendi, I., Allen, B., 2022. Pyrolysis of polyolefin plastic waste and potential applications in asphalt road construction: a technical review. *Resour. Conserv. Recycl.* 180, 106213. <https://doi.org/10.1016/J.RESCONREC.2022.106213>.
- Al-Salem, S.M., Dutta, A., 2021. Wax recovery from the pyrolysis of virgin and waste plastics. *Ind. Eng. Chem. Res.* 60, 8301–8309. https://doi.org/10.1021/ACS.IEGR.1C01176/ASSET/IMAGES/LARGE/IE1C01176_0004.JPEG.
- Al-Salem, S.M., Yang, Y., Wang, J., Leeke, G.A., 2020. Pyro-oil and wax recovery from reclaimed plastic waste in a continuous Auger pyrolysis reactor. *Energies* 13, 2040. <https://doi.org/10.3390/en13082040>.
- Albuquerque, M.G.E., Torres, C.A.V., Reis, M.A.M., 2010. Polyhydroxyalkanoate (PHA) production by a mixed microbial culture using sugar molasses: effect of the influent substrate concentration on culture selection. *Water Res.* 44, 3419–3433. <https://doi.org/10.1016/J.WATRES.2010.03.021>.
- Alvarez, H.M., 2003. Relationship between β -oxidation pathway and the hydrocarbon-degrading profile in actinomycetes bacteria. *Int. Biodeterior. Biodegradation* 52, 35–42. [https://doi.org/10.1016/S0964-8305\(02\)00120-8](https://doi.org/10.1016/S0964-8305(02)00120-8).
- Behera, I.D., Basak, G., Kumar, R.R., Sen, R., Meikap, B.C., 2020. Treatment of petroleum refinery sludge by petroleum degrading bacterium *Stenotrophomonas pavanii* IRB19 as an efficient novel technology. *J. Environ. Sci. Heal. Part A* 56, 226–239. <https://doi.org/10.1080/10934529.2020.1866924>.
- Behera, S., Priyadarshane, M., Vandana, Das, S., 2022. Polyhydroxyalkanoates, the bioplastics of microbial origin: properties, biochemical synthesis, and their applications. *Chemosphere* 294, 133723. <https://doi.org/10.1016/J.CHEMOSPHERE.2022.133723>.
- Bhattacharya, S., Das, A., Srividya, S., Prakruti, P.A., Priyanka, N., Sushmitha, B., 2020. Prospects of *Stenotrophomonas pavanii* DB1 in diesel utilization and reduction of its phytotoxicity on *Vigna radiata*. *Int. J. Environ. Sci. Technol.* 17, 445–454. <https://doi.org/10.1007/S13762-019-02302-W/FIGURES/5>.

- Brandl, H., Gross, R.A., Lenz, R.W., Fuller, R.C., 1988. *Pseudomonas oleovorans* as a source of poly(β -hydroxyalkanoates) for potential applications as biodegradable polyesters. *Appl. Environ. Microbiol.* 54, 1977–1982. <https://doi.org/10.1128/AEM.54.8.1977-1982.1988>.
- Bustamante, D., Tortajada, M., Ramon, D., Rojas, A., 2019. Camelina oil as a promising substrate for mcl-PHA production in *Pseudomonas* sp. *Cultures. Appl. Food Biotechnol.* 6, 61–70. <https://doi.org/10.22037/AFB.V6I1.21635>.
- Byrne, E., Schaefer, L.G., Kulas, D.G., Ankathi, S.K., Putman, L.I., Codere, K.R., Schum, S. K., Shonnard, D.R., Techtmann, S.M., 2022. Pyrolysis-aided microbial biodegradation of high-density polyethylene plastic by environmental inocula enrichment cultures. *ACS Sustain. Chem. Eng.* 10, 2022–2033. <https://doi.org/10.1021/ACSSUSCHEMENG.1C05318/ASSET/IMAGES/LARGE/SCI05318.0009.JPEG>.
- Chamas, A., Moon, H., Zheng, J., Qiu, Y., Tabassum, T., Jang, J.H., Abu-Omar, M., Scott, S.L., Suh, S., 2020. Degradation rates of plastics in the environment. *ACS Sustain. Chem. Eng.* 8, 3494–3511. <https://doi.org/10.1021/ACSSUSCHEMENG.9B06635/ASSET/IMAGES/LARGE/SC9B06635.0009.JPEG>.
- Chen, Y., Li, C., Zhou, Z., Wen, J., You, X., Mao, Y., Lu, C., Huo, G., Jia, X., 2014. Enhanced biodegradation of alkane hydrocarbons and crude oil by mixed strains and bacterial community analysis. *Appl. Biochem. Biotechnol.* 172, 3433–3447. <https://doi.org/10.1007/S12010-014-0777-6/FIGURES/8>.
- Christopher, F.J., Senthil Kumar, P., Jayaraman, L., Rangasamy, G., 2023. Assessment of product distribution of plastic waste from catalytic pyrolysis process. *Fuel* 332, 126168. <https://doi.org/10.1016/j.fuel.2022.126168>.
- Clifton-García, B., González-Reynoso, O., Robledo-Ortiz, J.R., Villafaña-Rojas, J., González-García, Y., 2020. Forest soil bacteria able to produce homo and copolymers of polyhydroxyalkanoates from several pure and waste carbon sources. *Lett. Appl. Microbiol.* 70, 300–309. <https://doi.org/10.1111/LAM.13272>.
- Cortes-Tolalpa, L., Jiménez, D.J., de Lima Brossi, M.J., Salles, J.F., van Elsland, J.D., 2016. Different inocula produce distinctive microbial consortia with similar lignocellulose degradation capacity. *Appl. Microbiol. Biotechnol.* 100, 7713–7725. <https://doi.org/10.1007/S00253-016-7516-6/TABLES/2>.
- Davis, R., Kataria, R., Cerrone, F., Woods, T., Kenny, S., O'Donovan, A., Guzik, M., Shaikh, H., Duane, G., Gupta, V.K., Tuohy, M.G., Padamatti, R.B., Casey, E., O'Connor, K.E., 2013. Conversion of grass biomass into fermentable sugars and its utilization for medium chain length polyhydroxyalkanoate (mcl-PHA) production by *Pseudomonas* strains. *Bioresour. Technol.* 150, 202–209. <https://doi.org/10.1016/J.BIORTECH.2013.10.001>.
- Deng, M.C., Li, J., Hong, Y.H., Xu, X.M., Chen, W.X., Yuan, J.P., Peng, J., Yi, M., Wang, J. H., 2016. Characterization of a novel biosurfactant produced by marine hydrocarbon-degrading bacterium *Achromobacter* sp. HZ01. *J. Appl. Microbiol.* 120, 889–899. <https://doi.org/10.1111/JAM.13065>.
- Deng, M.C., Li, J., Liang, F.R., Yi, M., Xu, X.M., Yuan, J.P., Peng, J., Wu, C.F., Wang, J.H., 2014. Isolation and characterization of a novel hydrocarbon-degrading bacterium *Achromobacter* sp. HZ01 from the crude oil-contaminated seawater at the Daya Bay, southern China. *Mar. Pollut. Bull.* 83, 79–86. <https://doi.org/10.1016/J.MARPOLBUL.2014.04.018>.
- Dragosits, M., Mattanovich, D., 2013. Adaptive laboratory evolution - principles and applications for biotechnology. *Microb. Cell Fact.* 12, 1–17. <https://doi.org/10.1186/1475-2859-12-64/TABLES/2>.
- European Bioplastics, e.V., 2023. Bioplastics market development update 2023 [WWW Document]. URL <https://www.european-bioplastics.org/bioplastics-market-development-update-2023-2/>, 8.21.24.
- European Commission, 2020. Circular economy action plan [WWW Document]. URL https://ec.europa.eu/environment/strategy/circular-economy-action-plan_en. (Accessed 3 July 2022).
- Feng, L., Wang, W., Cheng, J., Ren, Y., Zhao, G., Gao, C., Tang, Y., Liu, X., Han, W., Peng, X., Liu, R., Wang, L., 2007. Genome and proteome of long-chain alkane degrading *Geobacillus thermodenitrificans* NG80-2 isolated from a deep-subsurface oil reservoir. *Proc. Natl. Acad. Sci. U. S. A.* 104, 5602–5607. https://doi.org/10.1073/PNAS.0609650104/SUPPL_FILE/INDEX.HTML.
- Fenibo, E.O., Selvarajan, R., Abia, A.L.K., Matambo, T., 2023. Medium-chain alkane biodegradation and its link to some unifying attributes of alkB genes diversity. *Sci. Total Environ.* 877, 162951. <https://doi.org/10.1016/J.SCITOTENV.2023.162951>.
- García, J.M., Robertson, M.L., 2017. The future of plastics recycling. *Science* 358, 870–872. https://doi.org/10.1126/SCIENCE.AAQ0324/ASSET/53AC3A00-0BBA-41D7-A05A-BE986DAF5476/ASSETS/GRAPHIC/358_870_F1.JPEG.
- Gargouri, B., Contreras, M., del, M., Ammar, S., Segura-Carretero, A., Bouaziz, M., 2017. Biosurfactant production by the crude oil degrading *Stenotrophomonas* sp. B-2: chemical characterization, biological activities and environmental applications. *Environ. Sci. Pollut. Res.* 24, 3769–3779. <https://doi.org/10.1007/S11356-016-8064-4/FIGURES/5>.
- Gregory, G.J., Wang, C., Sadula, S., Koval, S., Lobo, R.F., Vlachos, D.G., Papoutsakis, E. T., 2023. Polyethylene valorization by combined chemical catalysis with bioconversion by plastic-enriched microbial consortia. *ACS Sustain. Chem. Eng.* 11, 3494–3505. <https://doi.org/10.1021/acssuschemeng.2c07461>.
- Guzik, M.W., Duane, G.F., Kenny, S.T., Casey, E., Mielcarek, P., Wojnarowska, M., O'Connor, K.E., 2022. A polyhydroxyalkanoates bioprocess improvement case study based on four fed-batch feeding strategies. *Microb. Biotechnol.* 15, 996–1006. <https://doi.org/10.1111/1751-7915.13879>.
- Guzik, M.W., Kenny, S.T., Duane, G.F., Casey, E., Woods, T., Babu, R.P., Nikodinovic-Runic, J., Murray, M., O'Connor, K.E., 2014. Conversion of post consumer polyethylene to the biodegradable polymer polyhydroxyalkanoate. *Appl. Microbiol. Biotechnol.* 98, 4223–4232. <https://doi.org/10.1007/s00253-013-5489-2>.
- Guzik, M.W., Nitkiewicz, T., Wojnarowska, M., Soltysik, M., Kenny, S.T., Babu, R.P., Best, M., O'Connor, K.E., 2021. Robust process for high yield conversion of non-degradable polyethylene to a biodegradable plastic using a chemo-biotechnological approach. *Waste Manag.* 135, 60–69. <https://doi.org/10.1016/J.WASMAN.2021.08.030>.
- Hahn, T., Alzate, M.O., Leonhardt, S., Tamang, P., Zibek, S., 2024. Current trends in medium-chain-length polyhydroxyalkanoates: microbial production, purification, and characterization. *Eng. Life Sci.* 24, 2300211. <https://doi.org/10.1002/ELSC.202300211>.
- Hassanshahian, M., Ahmadinejad, M., Tebyanian, H., Kariminik, A., 2013. Isolation and characterization of alkane degrading bacteria from petroleum reservoir waste water in Iran (Kerman and Tehran provenances). *Mar. Pollut. Bull.* 73, 300–305. <https://doi.org/10.1016/J.MARPOLBUL.2013.05.002>.
- Hua, F., Wang, H.Q., 2014. Uptake and trans-membrane transport of petroleum hydrocarbons by microorganisms. *Biotechnol. Equip.* 28, 165–175. <https://doi.org/10.1080/13102818.2014.906136>.
- Hua, F., Wang, H.Q., Li, Y., Zhao, Y.C., 2013. Trans-membrane transport of n-octadecane by *Pseudomonas* sp. DG17. *J. Microbiol.* 51, 791–799. <https://doi.org/10.1007/S12275-013-3259-6/METRICS>.
- Ji, Y., Mao, G., Wang, Y., Bartlam, M., 2013. Structural insights into diversity and n-alkane biodegradation mechanisms of alkane hydroxylases. *Front. Microbiol.* 58. <https://doi.org/10.3389/FMICB.2013.00058>, 0.
- Johnston, B., Jiang, G., Hill, D., Adams, G., Kwiecień, I., Zięba, M., Sikorska, W., Green, M., Kowalczyk, M., Radecka, I., 2017. The molecular level characterization of biodegradable polymers originated from polyethylene using non-oxygenated polyethylene wax as a carbon source for polyhydroxyalkanoate production. *Bioengineering* 4, 73. <https://doi.org/10.3390/bioengineering4030073>.
- Justice, N.B., Szczesnak, A., Hazen, T.C., Arkin, A.P., 2017. Environmental selection, dispersal, and organism interactions shape community assembly in high-throughput enrichment culturing. *Appl. Environ. Microbiol.* 83. <https://doi.org/10.1128/AEM.01253-17>.
- Kaczorek, E., Salek, K., Guzik, U., Dudzińska-Bajorek, B., 2013. Cell surface properties and fatty acids composition of *Stenotrophomonas maltophilia* under the influence of hydrophobic compounds and surfactants. *N. Biotechnol.* 30, 173–182. <https://doi.org/10.1016/J.NBT.2012.09.003>.
- Kazemzadeh, S., Naghavi, N.S., Emami-Karvani, Z., Emtiazi, G., Fouladgar, M., 2020. Production of glycolipid biosurfactant during crude oil degradation by the novel indigenous isolated *Achromobacter kerstersii* LMG3441. *Water Sci. Technol.* 82, 2134–2147. <https://doi.org/10.2166/WST.2020.474>.
- Khamkong, T., Penkhrue, W., Lumyong, S., 2022. Optimization of production of polyhydroxyalkanoates (PHAs) from newly isolated ensifer sp. strain HD34 by response surface methodology. *Process* 10. <https://doi.org/10.3390/PR10081632>, 1632 10, 1632.
- Konstantinidis, D., Pereira, F., Geissen, E., Grkovska, K., Kafkia, E., Jouhten, P., Kim, Y., Devendran, S., Zimmermann, M., Patil, K.R., 2021. Adaptive laboratory evolution of microbial co-cultures for improved metabolite secretion. *Mol. Syst. Biol.* 17. <https://doi.org/10.1525/msb.202010189>.
- Kourmentza, C., Plácido, J., Venetsaneas, N., Burniol-Figols, A., Varrone, C., Gavala, H. N., Reis, M.A.M., 2017. Recent advances and challenges towards sustainable polyhydroxyalkanoate (PHA) production. *Bioeng.* 4, 2017. <https://doi.org/10.3390/BIOENGINEERING4020055>. Page 55 4, 55.
- Krupa, I., Miková, G., Luyt, A.S., 2007. Phase change materials based on low-density polyethylene/paraffin wax blends. *Eur. Polym. J.* 43, 4695–4705. <https://doi.org/10.1016/J.EURPOLYMJ.2007.08.022>.
- Lalejini, A., Dolson, E., Vostinar, A.E., Zaman, L., 2022. Artificial selection methods from evolutionary computing show promise for directed evolution of microbes. *Elife* 11, e79665. <https://doi.org/10.7554/eLife.79665>.
- Li, J., Wang, Y., Zhou, W., Chen, W., Deng, M., Zhou, S., 2020. Characterization of a new biosurfactant produced by an effective pyrene-degrading *Achromobacter* species strain AC15. *Int. Biodeterior. Biodegradation* 152, 104959. <https://doi.org/10.1016/J.IBIDOD.2020.104959>.
- Li, Y., Tian, Y., Hao, Z., Ma, Y., 2020. Complete genome sequence of the aromatic-hydrocarbon-degrading bacterium *Achromobacter xylosoxidans* DN002. *Arch. Microbiol.* 202, 2849–2853. <https://doi.org/10.1007/S00203-020-01977-X/TABLES/2>.
- Liu, H., Xu, J., Liang, R., Liu, J., 2014. Characterization of the medium- and long-chain n-alkanes degrading *Pseudomonas aeruginosa* strain SJTD-1 and its alkane hydroxylase genes. *PLoS One* 9, e105506. <https://doi.org/10.1371/JOURNAL.PONE.0105506>.
- Liu, R., Chen, Y., Tian, Z., Mao, Z., Cheng, H., Zhou, H., Wang, W., 2019. Enhancing microbial community performance on acid resistance by modified adaptive laboratory evolution. *Bioresour. Technol.* 287, 121416. <https://doi.org/10.1016/J.BIORTECH.2019.121416>.
- Mahato, R.P., Kumar, S., Singh, P., 2023. Production of polyhydroxyalkanoates from renewable resources: a review on prospects, challenges and applications. *Arch. Microbiol.* 205, 1–31. <https://doi.org/10.1007/S00203-023-03499-8>, 2023 2055.
- Mahendhran, K., Arthanari, A., Dheenadayalan, B., Ramanathan, M., 2018. Bioconversion of oily bilge waste to polyhydroxybutyrate (PHB) by marine *Ochrobactrum intermedium*. *Bioresour. Technol. Reports* 4, 66–73. <https://doi.org/10.1016/J.BITEB.2018.08.013>.
- Massot, F., Bernard, N., Alvarez, L.M.M., Martorell, M.M., Mac Cormack, W.P., Ruberto, L.A.M., 2022. Microbial associations for bioremediation. What does “microbial consortia” mean? *Appl. Microbiol. Biotechnol.* 1067 (106), 2283–2297. <https://doi.org/10.1007/S00253-022-11864-8>, 2022.
- McEnany, J., Good, B.H., 2024. Predicting the first steps of evolution in randomly assembled communities. *bioRxiv*. <https://doi.org/10.1101/2023.12.15.571925> [Preprint].

- Mihreteab, M., Stubblefield, B.A., Gilbert, E.S., 2021. Enhancing polypropylene bioconversion and lipogenesis by *Yarrowia lipolytica* using a chemical/biological hybrid process. *J. Biotechnol.* 332, 94–102. <https://doi.org/10.1016/j.jbiotec.2021.03.015>.
- Mihreteab, M., Stubblefield, B.A., Gilbert, E.S., 2019. Microbial bioconversion of thermally depolymerized polypropylene by *Yarrowia lipolytica* for fatty acid production. *Appl. Microbiol. Biotechnol.* 103, 7729–7740. <https://doi.org/10.1007/s00253-019-09999-2>.
- Mir, M., Ghasemirad, S., 2022. Phase inversion emulsification of paraffin oil/polyethylene wax blend in water: a comparison between mixed monomeric and monomeric/gemini surfactant systems. *J. Mol. Liq.* 359, 119315. <https://doi.org/10.1016/j.molliq.2022.119315>.
- Miri, M., Bambai, B., Tabandeh, F., Sadeghizadeh, M., Kamali, N., 2010. Production of a recombinant alkane hydroxylase (AlkB2) from *Alcanivorax borkumensis*. *Biotechnol. Lett.* 32, 497–502. <https://doi.org/10.1007/s10529-009-0177-0/FIGURES/2>.
- Mohanty, S., Jasmine, J., Mukherji, S., 2013. Practical considerations and challenges involved in surfactant enhanced bioremediation of oil. *BioMed Res. Int.* 2013, 328608. <https://doi.org/10.1155/2013/328608>.
- Montazer, Z., Habibi-Najafi, M.B., Mohebbi, M., Oromiehei, A., 2018. Microbial degradation of UV-pretreated low-density polyethylene films by novel polyethylene-degrading bacteria isolated from plastic-dump soil. *J. Polym. Environ.* 26, 3613–3625. <https://doi.org/10.1007/s10924-018-1245-0>.
- Myers, M.E., Stollsteimer, J., Wims, A.M., 1975. Determination of hydrocarbon-type distribution and hydrogen/carbon ratio of gasoline by nuclear magnetic resonance spectrometry. *Anal. Chem.* 47, 2010–2015. <https://doi.org/10.1021/ac60362a020>.
- Nygaard, D., Yashchuk, O., Hermida, É.B., 2023. Polyhydroxyalkanoates (PHAs) production from residual glycerol by wild type *Cupriavidus necator*. *Waste and Biomass Valorization* 14, 1489–1496. <https://doi.org/10.1007/s12649-022-01979-4/TABLES/2>.
- OECD, 2022. Global Plastics Outlook: Economic Drivers, Environmental Impacts and Policy Options, Global Plastics Outlook. OECD Publishing, Paris. <https://doi.org/10.1787/de747aef-en>.
- Parajuli, S., Alazzam, O., Wang, M., Mota, L.C., Adhikari, S., Wicks, D., Ureña-Benavides, E.E., 2020. Surface properties of cellulose nanocrystal stabilized crude oil emulsions and their effect on petroleum biodegradation. *Colloids Surfaces A Physicochem. Eng. Asp.* 596, 124705. <https://doi.org/10.1016/j.colsurfa.2020.124705>.
- Park, C., Shin, B., Jung, J., Lee, Y., Park, W., 2017. Metabolic and stress responses of *Acinetobacter oleivorans* DR1 during long-chain alkane degradation. *Microb. Biotechnol.* 10, 1809–1823. <https://doi.org/10.1111/1751-7915.12852>.
- Park, H., He, H., Yan, X., Liu, X., Scrutton, N.S., Chen, G.Q., 2024. PHA is not just a bioplastic. *Biotechnol. Adv.* 71, 108320. <https://doi.org/10.1016/j.biotechadv.2024.108320>.
- Pereira, J.R., Araújo, D., Marques, A.C., Neves, L.A., Grandfils, C., Sevrin, C., Alves, V.D., Fortunato, E., Reis, M.A.M., Freitas, F., 2019. Demonstration of the adhesive properties of the medium-chain-length polyhydroxyalkanoate produced by *Pseudomonas chlororaphis* subsp. *aurantiaca* from glycerol. *Int. J. Biol. Macromol.* 122, 1144–1151. <https://doi.org/10.1016/j.ijbiomac.2018.09.064>.
- Piccardi, P., Vessman, B., Mitri, S., 2019. Toxicity drives facilitation between 4 bacterial species. *Proc. Natl. Acad. Sci. U. S. A.* 116, 15979–15984. https://doi.org/10.1073/pnas.1906172116/SUPPL_FILE/PNAS.1906172116.SD03.XLSX.
- PlasticsEurope, 2023. Plastics – the fast facts 2023 [WWW Document]. URL: <https://plasticseurope.org/knowledge-hub/plastics-the-fast-facts-2023/>, 9.2.24.
- Portnoy, V.A., Bezdán, D., Zengler, K., 2011. Adaptive laboratory evolution — harnessing the power of biology for metabolic engineering. *Curr. Opin. Biotechnol.* 22, 590–594. <https://doi.org/10.1016/j.copbio.2011.03.007>.
- Radecka, I., Irorere, V., Jiang, G., Hill, D., Williams, C., Adamus, G., Kwiecień, M., Marek, A.A., Zawadiak, J., Johnston, B., Kowalczyk, M., 2016. Oxidized polyethylene wax as a potential carbon source for PHA production. *Materials* 9, 367. <https://doi.org/10.3390/ma9050367>.
- Rojo, F., 2010. Enzymes for aerobic degradation of alkanes. *Handb. Hydrocarb. Lipid Microbiol.* 781–797. https://doi.org/10.1007/978-3-540-77587-4_59.
- Roux, M., Varrone, C., 2021. Assessing the economic viability of the plastic biorefinery concept and its contribution to a more circular plastic sector. *Polym* 13. <https://doi.org/10.3390/POLYM13223883>. Page 3883 13, 3883.
- Sarwar, B., Rahman, Z., 2021. Central composite designs and their applications in pharmaceutical product development. *Des. Exp. Pharm. Prod. Dev. Vol. I Basics Fundam. Princ.* 1, 63–76. https://doi.org/10.1007/978-981-33-4717-5_6/TABLES/4.
- Sayyed, R.Z., Shaikh, S.S., Wani, S.J., Rehman, M.T., Al Ajmi, M.F., Haque, S., Enshasy, H.A. El, 2021. Production of biodegradable polymer from agro-wastes in *Alcaligenes* sp. and *Pseudomonas* sp. *Mol* 26. <https://doi.org/10.3390/MOLECULES26092443>. Page 2443 26, 2443.
- Serafim, L.S., Lemos, P.C., Albuquerque, M.G.E., Reis, M.A.M., 2008. Strategies for PHA production by mixed cultures and renewable waste materials. *Appl. Microbiol. Biotechnol.* 81, 615–628. <https://doi.org/10.1007/s00253-008-1757-Y/TABLES/2>.
- Shapiro, T.N., Manucharova, N.A., Lobakova, E.S., 2022. Activity of alkanonooxygenase alkB genein strains of hydrocarbon-oxidizing bacteriaisolated from petroleum products. *Vavilov J. Genet. Breed.* 26, 575. <https://doi.org/10.18699/VJGB-22-70>.
- Sindhu, R., Ammu, B., Binod, P., Deepthi, S.K., Ramachandran, K.B., Soccol, C.R., Pandey, A., 2011. Production and characterization of poly-3-hydroxybutyrate from crude glycerol by *Bacillus sphaericus* NII 0838 and improving its thermal properties by blending with other polymers. *Brazilian Arch. Biol. Technol.* 54, 783–794. <https://doi.org/10.1590/S1516-89132011000400019>.
- Singh, S.N., Kumari, B., Mishra, S., 2012. Microbial degradation of alkanes. In: *Microbial Degradation of Xenobiotics*. Springer, Berlin, Heidelberg, pp. 439–469. https://doi.org/10.1007/978-3-642-23789-8_17.
- Tamboli, D.P., Kagalkar, A.N., Jadhav, M.U., Jadhav, J.P., Govindwar, S.P., 2010. Production of polyhydroxyhexadecanoic acid by using waste biomass of *Sphingobacterium* sp. ATM generated after degradation of textile dye Direct Red 5B. *Bioresour. Technol.* 101, 2421–2427. <https://doi.org/10.1016/j.biortech.2009.11.094>.
- Tekin, K., Akalin, M.K., Kadi, C., Karagöz, S., 2012. Catalytic degradation of waste polypropylene by pyrolysis. *J. Energy Inst.* 85, 150–155. <https://doi.org/10.1179/1743967112Z.00000000029>.
- Torres-Zapata, T., Lozano-Martinez, P., Martinez-Lorenzo, M.V., Buey, R.M., Martin-Sanchez, N., 2022. Hydrothermally processed polyethylene as starting point for fermentative production of triglycerides. *J. Environ. Chem. Eng.* 10, 108683. <https://doi.org/10.1016/j.jece.2022.108683>.
- Tzirtza, M., Papanikolaou, S., Chatzifragkou, A., Quilty, B., 2018. Waste fat biodegradation and biomodification by *Yarrowia lipolytica* and a bacterial consortium composed of *Bacillus* spp. and *Pseudomonas putida*. *Eng. Life Sci.* 18, 932–942. <https://doi.org/10.1002/ELSC.201800067>.
- Van Beilen, J.B., Funhoff, E.G., 2007. Alkane hydroxylases involved in microbial alkane degradation. *Appl. Microbiol. Biotechnol.* 74, 13–21. <https://doi.org/10.1007/S00253-006-0748-0/FIGURES/3>.
- Varrone, C., Skiadas, I.V., Gavala, H.N., 2018. Effect of hydraulic retention time on the modelling and optimization of joint 1,3 PDO and BuA production from 2G glycerol in a chemostat process. *Chem. Eng. J.* 347, 525–534. <https://doi.org/10.1016/j.cej.2018.04.071>.
- Venkateswar Reddy, M., Mawatari, Y., Onodera, R., Nakamura, Y., Yajima, Y., Chang, Y. C., 2017. Polyhydroxyalkanoates (PHA) production from synthetic waste using *Pseudomonas pseudoflava*: PHA synthase enzyme activity analysis from *P. pseudoflava* and *P. palleronii*. *Bioresour. Technol.* 234, 99–105. <https://doi.org/10.1016/j.biortech.2017.03.008>.
- Venkidesamy, K., Megharaj, M., 2016. Identification of electrode respiring, hydrocarbonoclastic bacterial strain *Stenotrophomonas maltophilia* MK2 highlights the untapped potential for environmental bioremediation. *Front. Microbiol.* 7, 229962. <https://doi.org/10.3389/fmicb.2016.01965/BIBTEX>.
- Welsing, G., Wolter, B., Hintzen, H.M.T., Tiso, T., Blank, L.M., 2021. Upcycling of hydrolyzed PET by microbial conversion to a fatty acid derivative. *Methods Enzymol.* 648, 391–421. <https://doi.org/10.1016/bs.mie.2020.12.025>.
- Wongwilaivalin, S., Laothanachareon, T., Mhuantong, W., Tangphatsornruang, S., Eurwilachitr, L., Igarashi, Y., Champreda, V., 2013. Comparative metagenomic analysis of microcosm structures and lignocellulolytic enzyme systems of symbiotic biomass-degrading consortia. *Appl. Microbiol. Biotechnol.* 97, 8941–8954. <https://doi.org/10.1007/s00253-013-4699-Y/FIGURES/6>.
- Wu, B., Xiu, J., Yu, L., Huang, L., Yi, L., Ma, Y., 2023. Degradation of crude oil in a coculture system of *Bacillus subtilis* and *Pseudomonas aeruginosa*. *Front. Microbiol.* 14, 1132831. <https://doi.org/10.3389/fmicb.2023.1132831/BIBTEX>.
- Yao, Y., Chau, E., Azimi, G., 2019. Supercritical fluid extraction for purification of waxes derived from polyethylene and polypropylene plastics. *Waste Manag.* 97, 131–139. <https://doi.org/10.1016/j.wasman.2019.08.003>.
- Yin, C.F., Nie, Y., Li, T., Zhou, N.Y., 2024. Alma involved in the long-chain n-alkane degradation pathway in *Acinetobacter baylyi* ADP1 is a Baeyer–Villiger monooxygenase. *Appl. Environ. Microbiol.* 90. https://doi.org/10.1128/AEM.01625-23/SUPPL_FILE/AEM.01625-23-S0001.DOCX.
- Zhang, X., Kong, D., Liu, X., Xie, H., Lou, X., Zeng, C., 2021. Combined microbial degradation of crude oil under alkaline conditions by *Acinetobacter baumannii* and *Talaromyces* sp. *Chemosphere* 273, 129666. <https://doi.org/10.1016/j.chemosphere.2021.129666>.
- Zwietering, M.H., Jongenburger, I., Rombouts, F.M., Van't Riet, K., 1990. Modeling of the bacterial growth curve. *Appl. Environ. Microbiol.* 56, 1875–1881. <https://doi.org/10.1128/AEM.56.6.1875-1881.1990>.